Di-Pions in Ultra-Peripheral Collisions at LHCb

Amanda Donohoe
LHCb Collaboration
Hard Probes
27/09/2024

Outline

- Introduction
- Motivation
- Structure in the di-pion invariant mass spectrum
- Conclusion

Introduction

Process of Interest

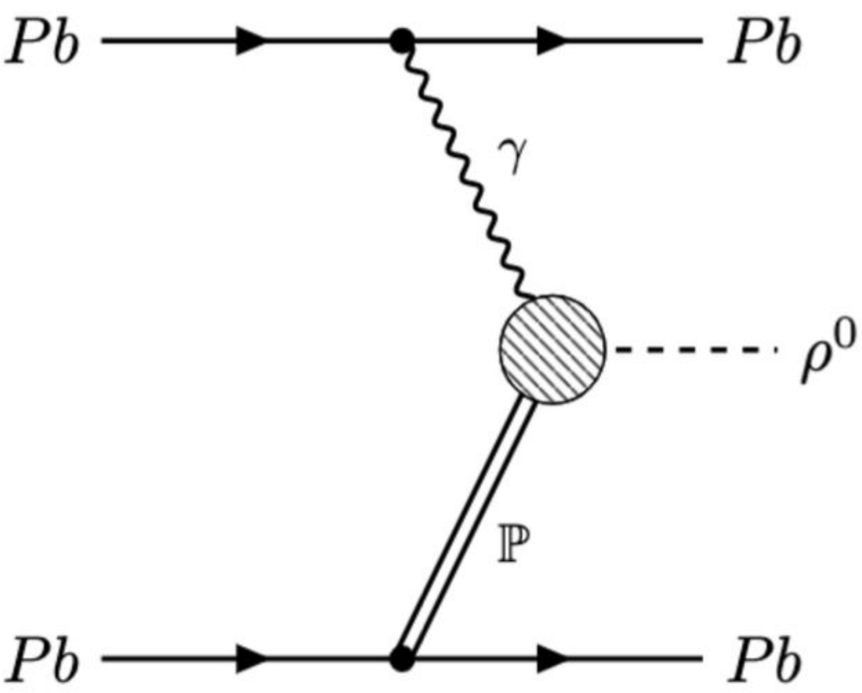

Process of Interest

Central Exclusive Production (CEP)

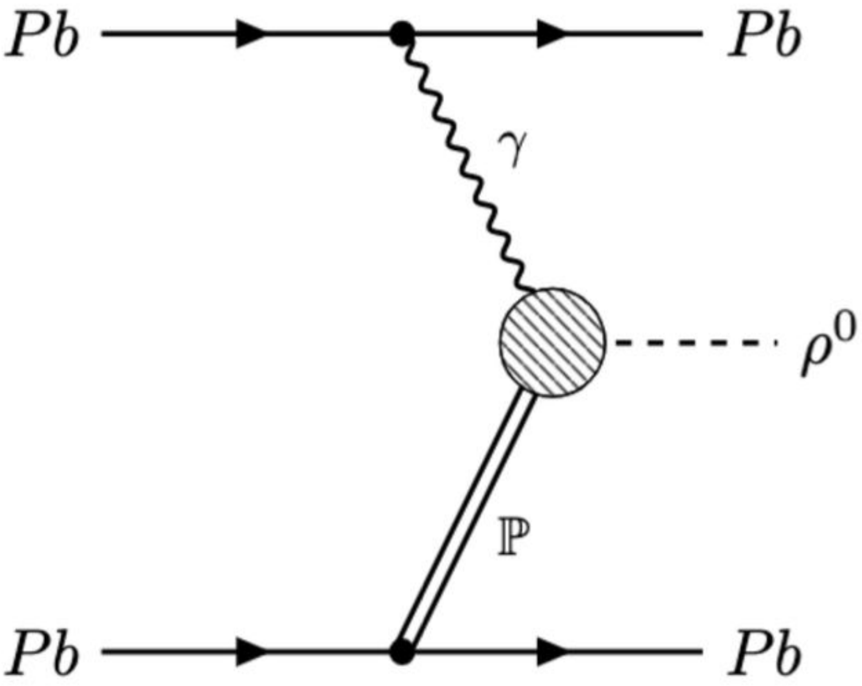

Process of Interest

Central Exclusive Production (CEP)

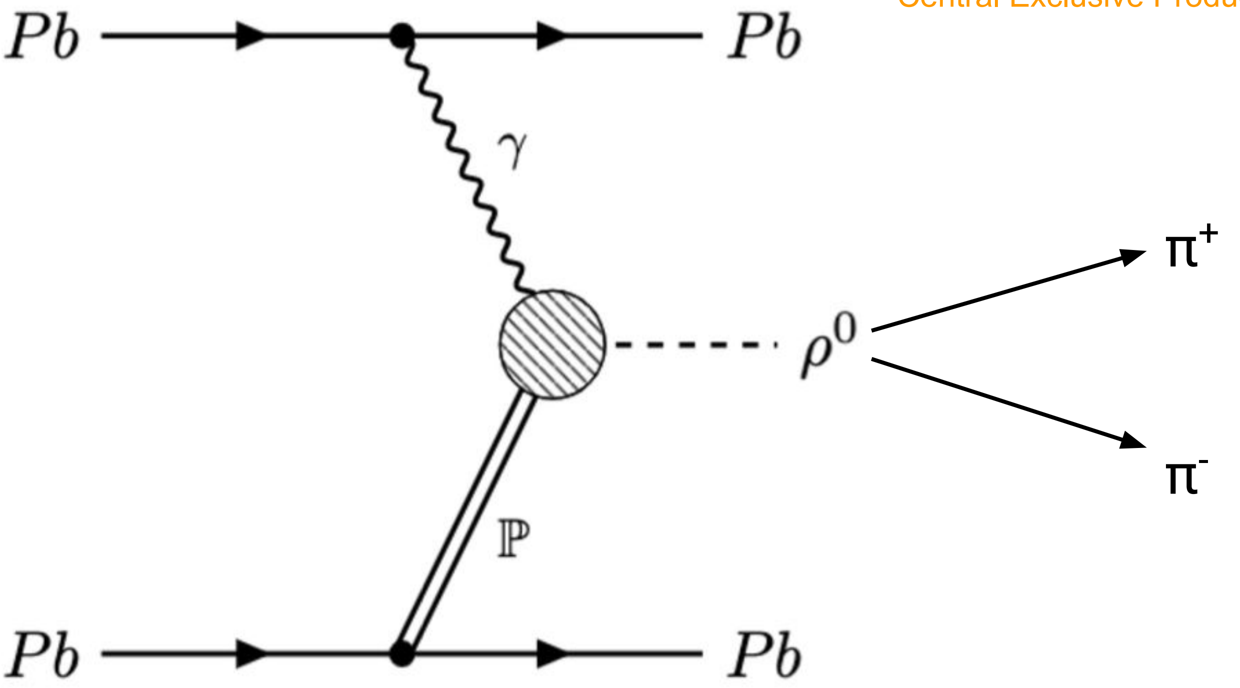

Process of Interest

Central Exclusive Production (CEP)

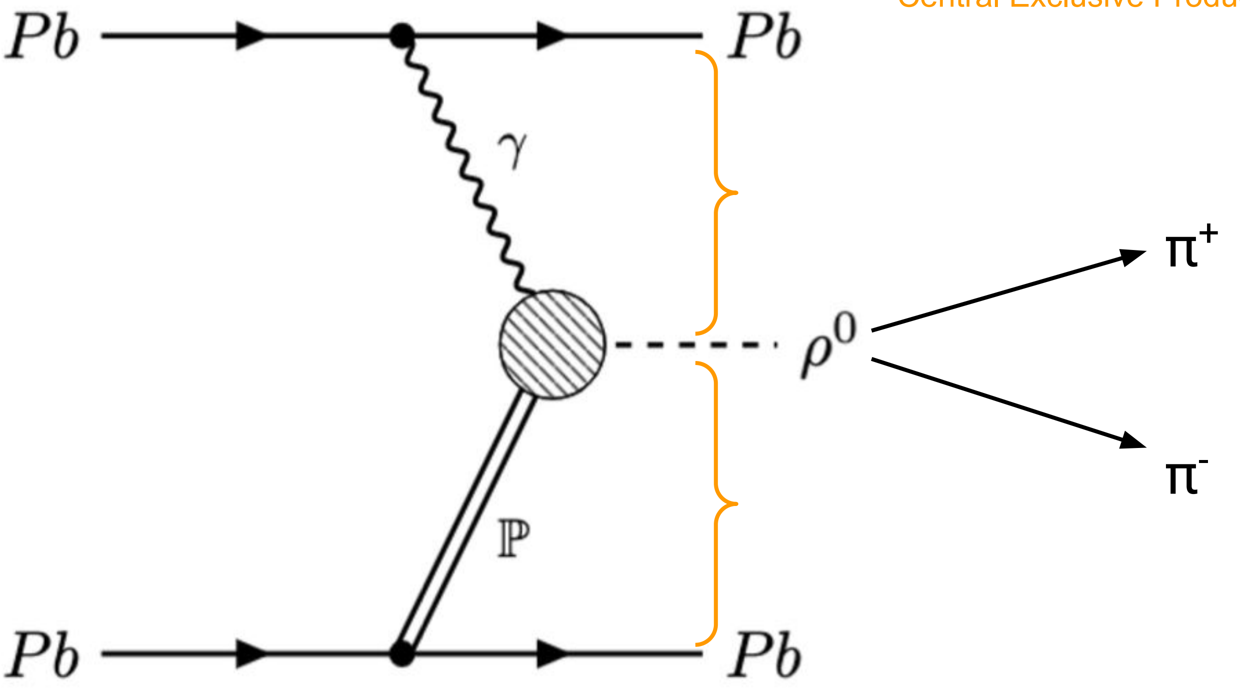

} = Rapidity Gap

Process of Interest

Central Exclusive Production (CEP)

Quasi-Real Photon

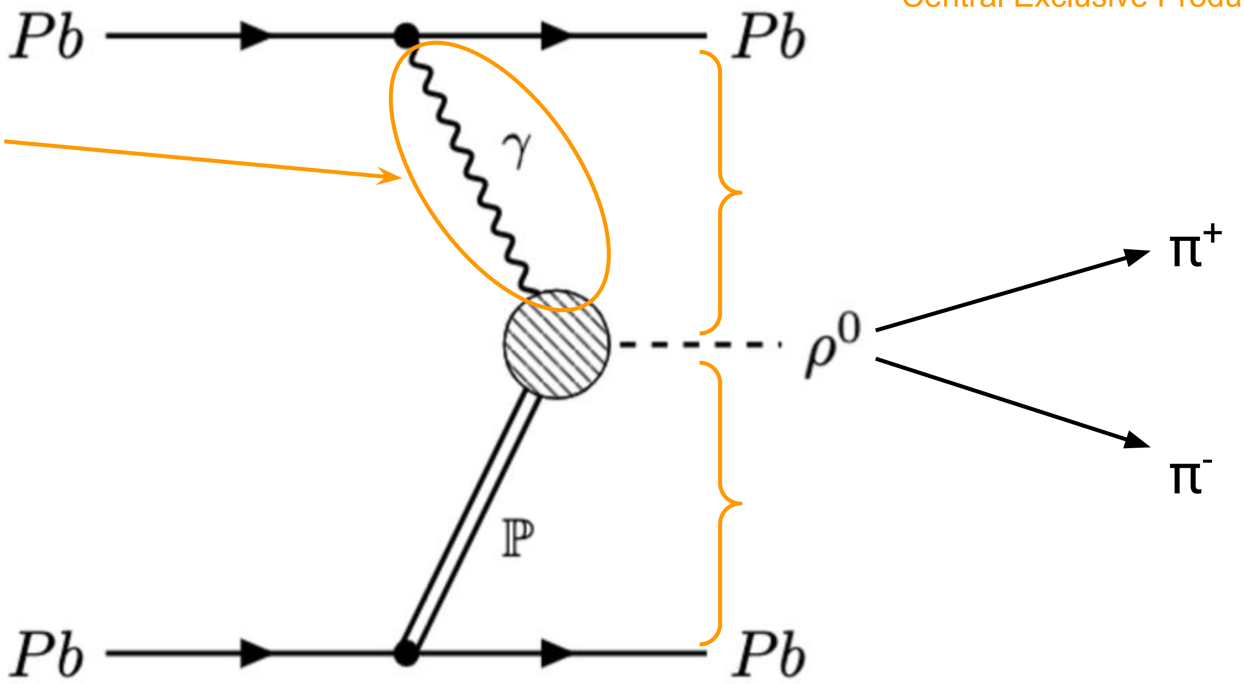

= Rapidity Gap

Process of Interest

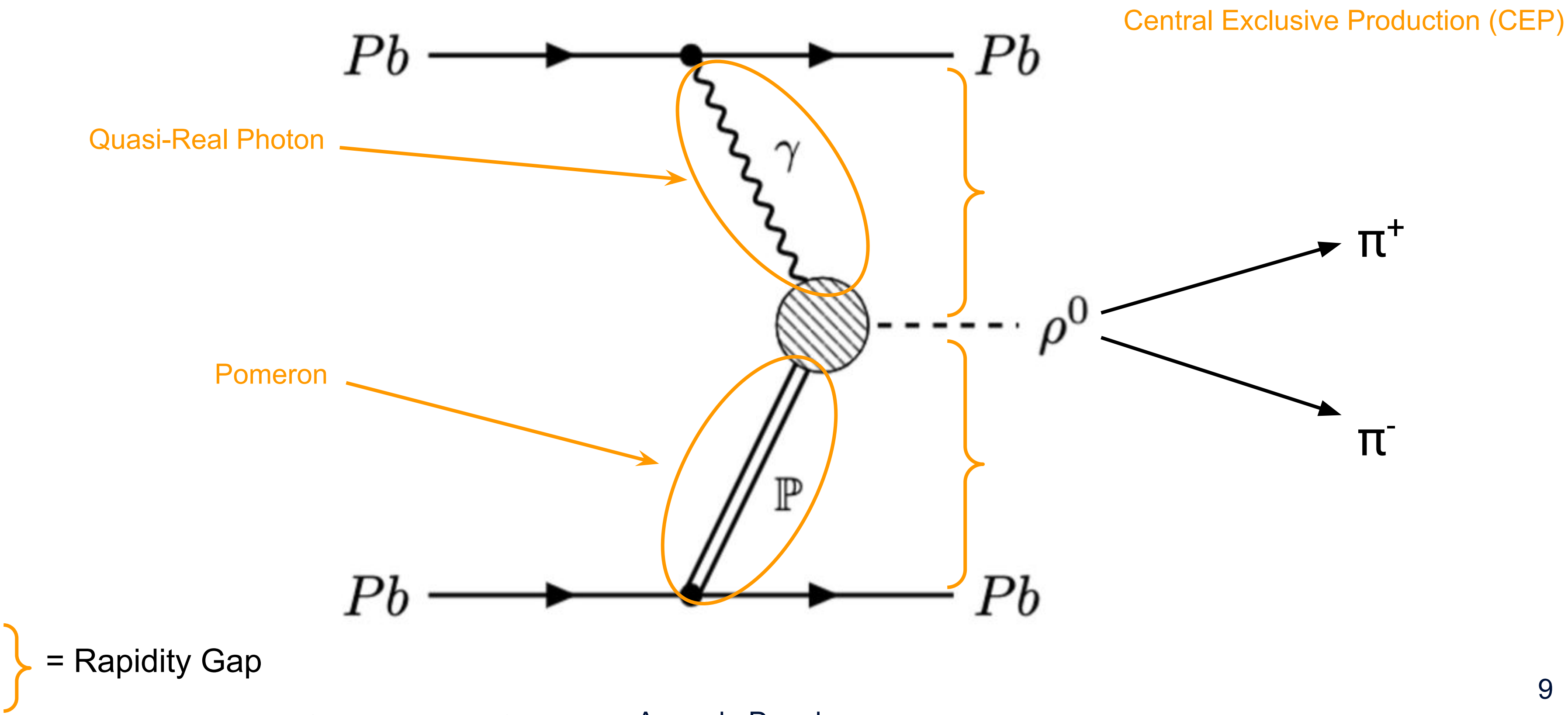

Ultra-Peripheral Collisions

Ultra-Peripheral Collisions

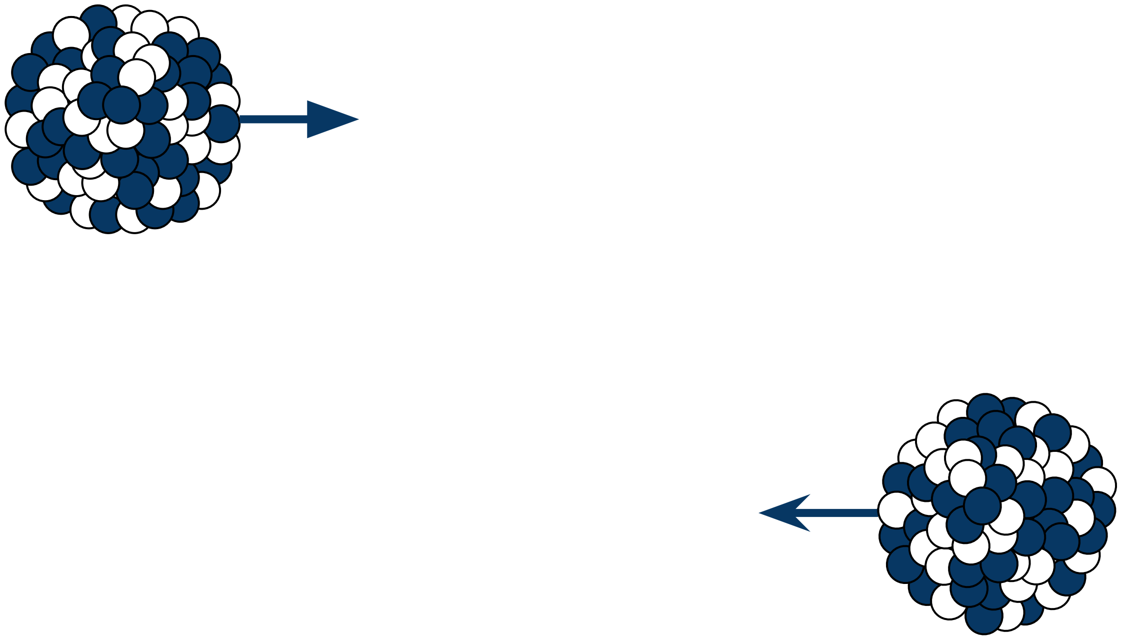

Ultra-Peripheral Collisions

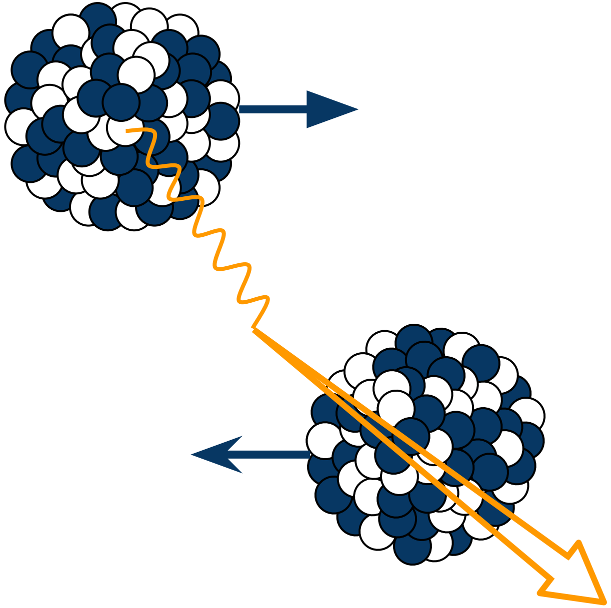

Ultra-Peripheral Collisions

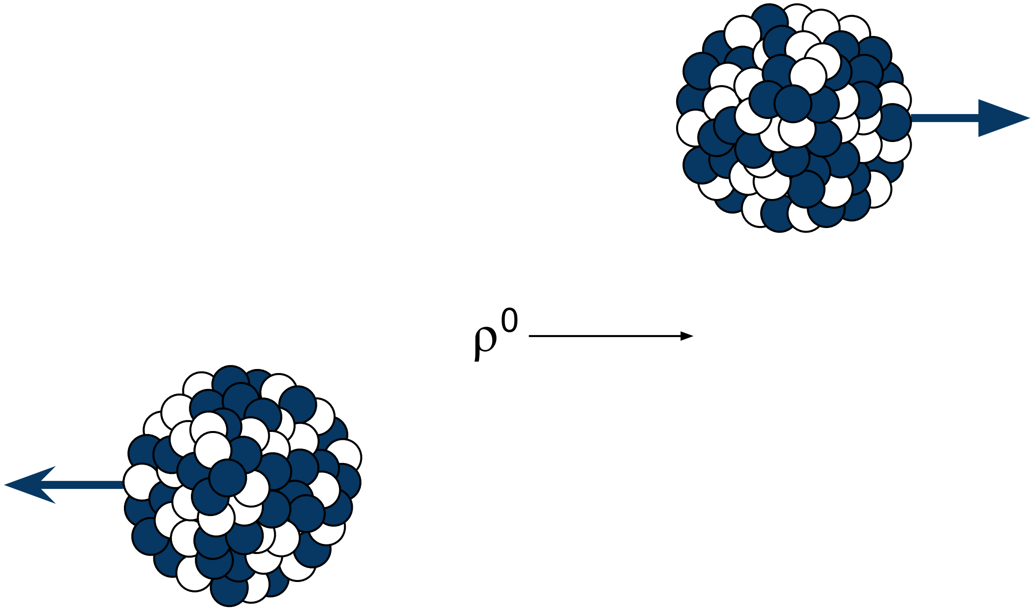

Ultra-Peripheral Collisions

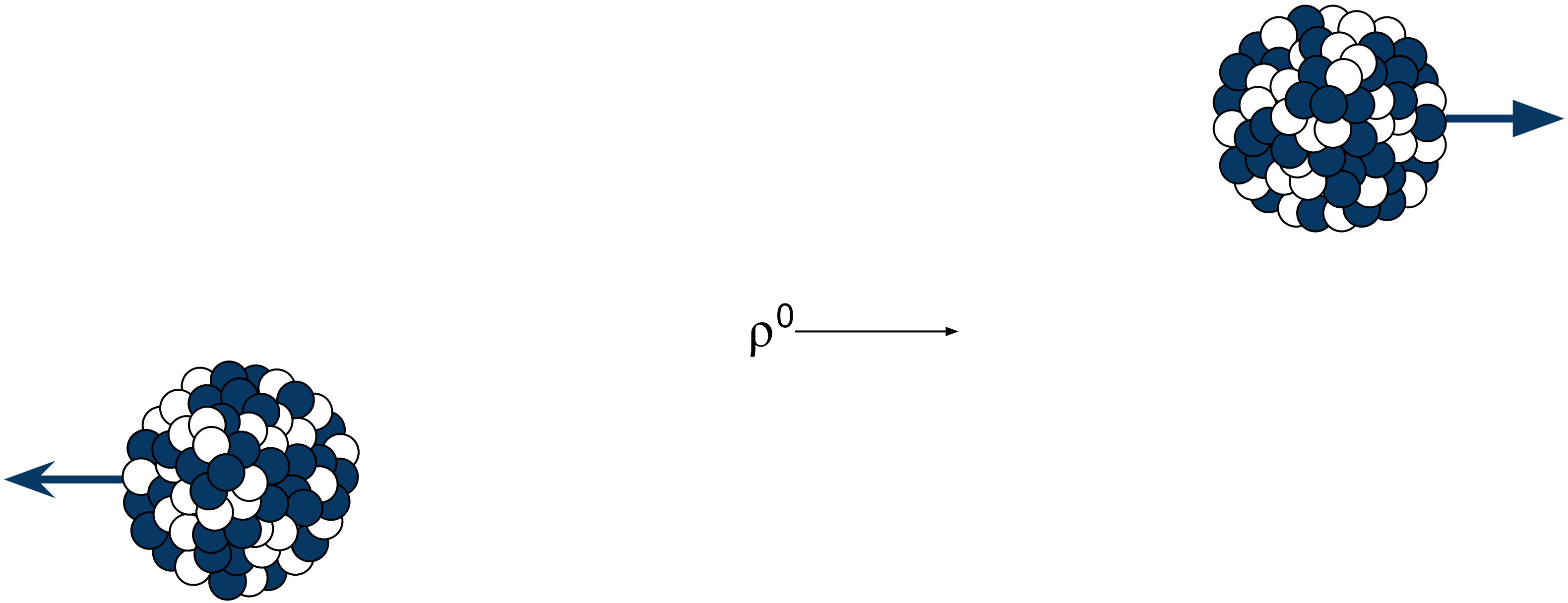

Ultra-Peripheral Collisions

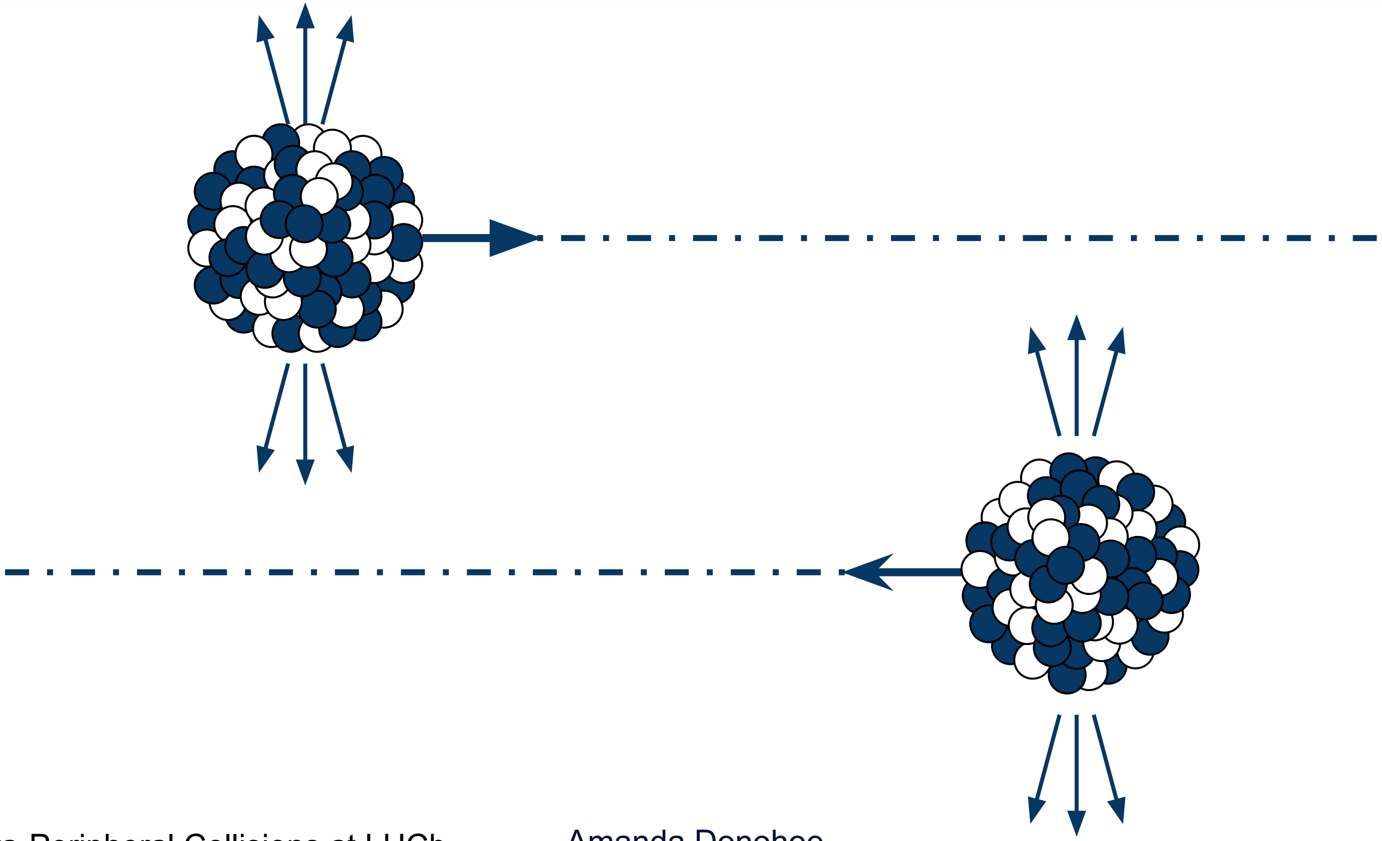

Ultra-Peripheral Collisions

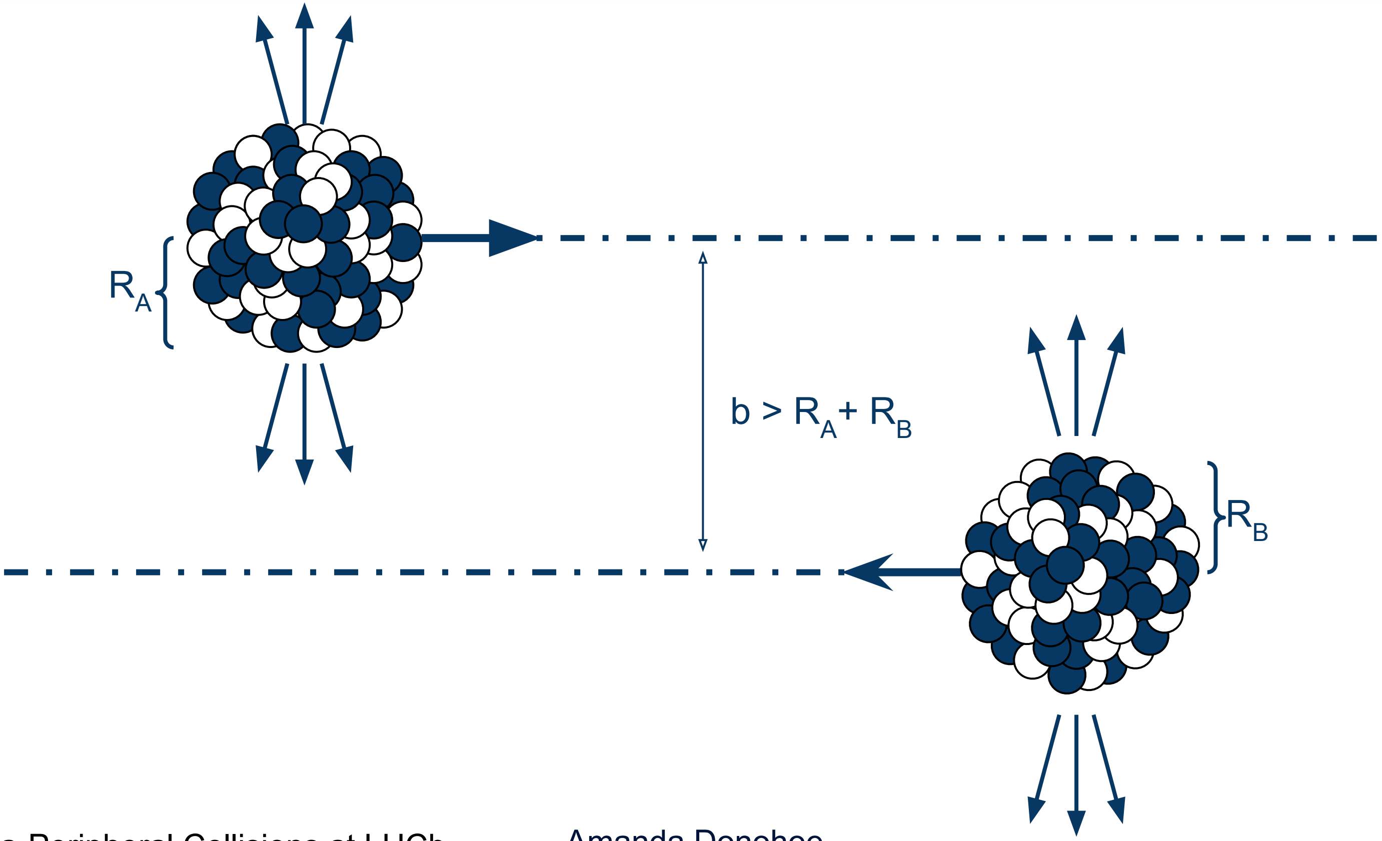

Ultra-Peripheral Collisions

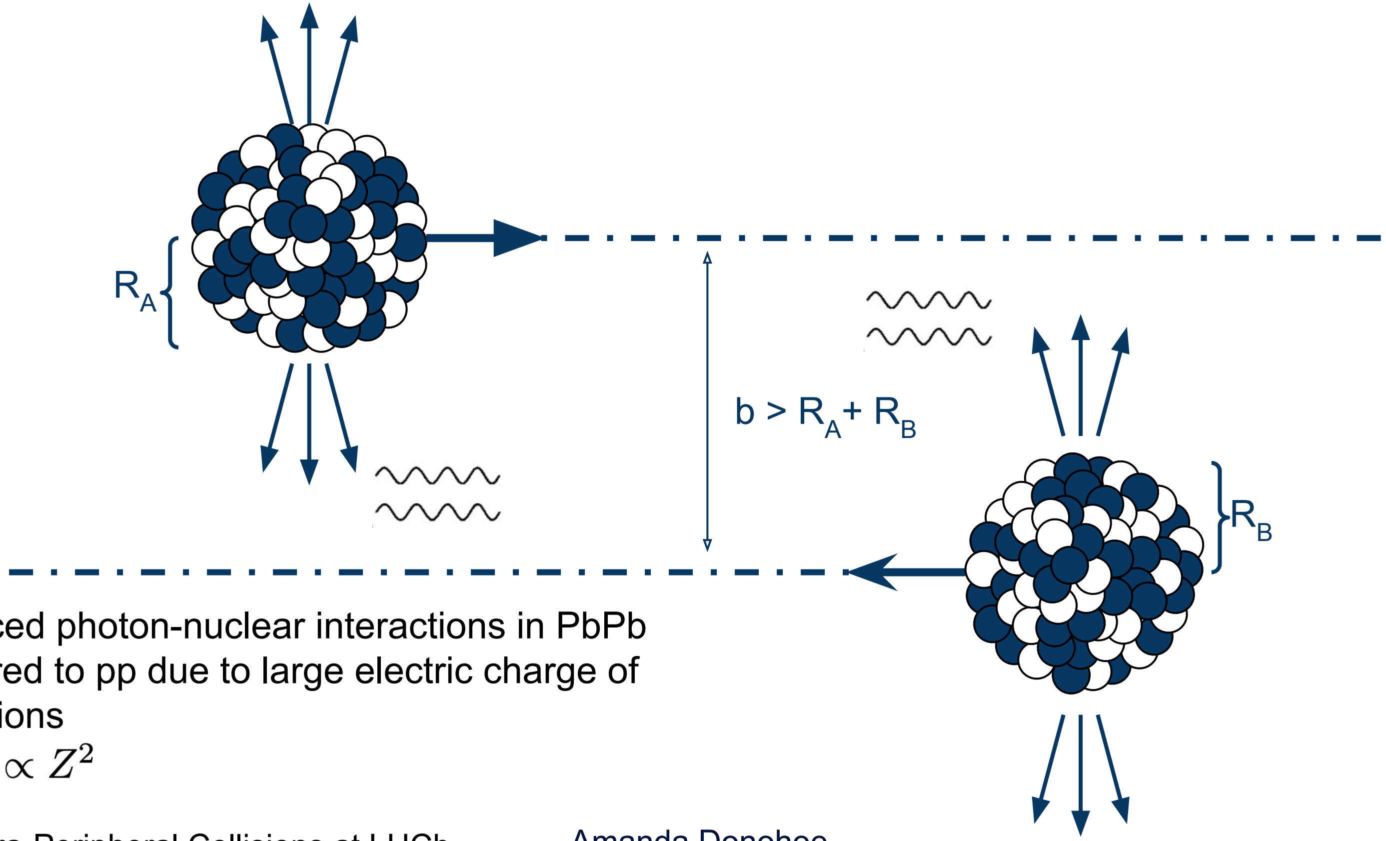

- Enhanced photon-nuclear interactions in PbPb compared to pp due to large electric charge of the Pb ions
  - $N_\gamma \propto Z^2$

Coherent vs Incoherent Interactions

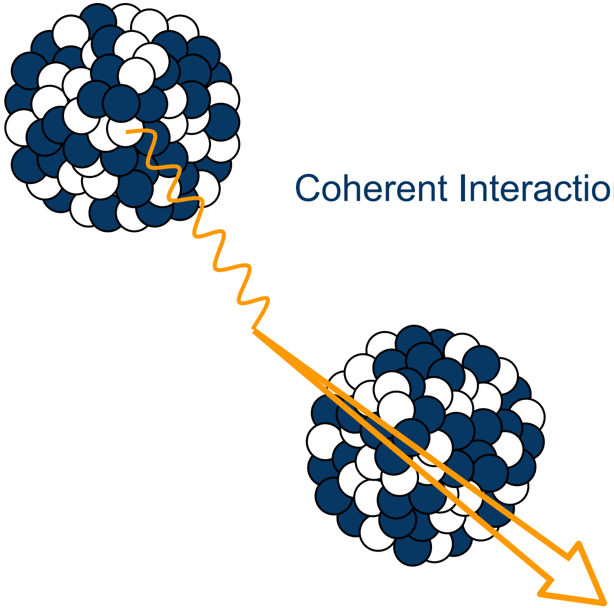

Coherent Interaction

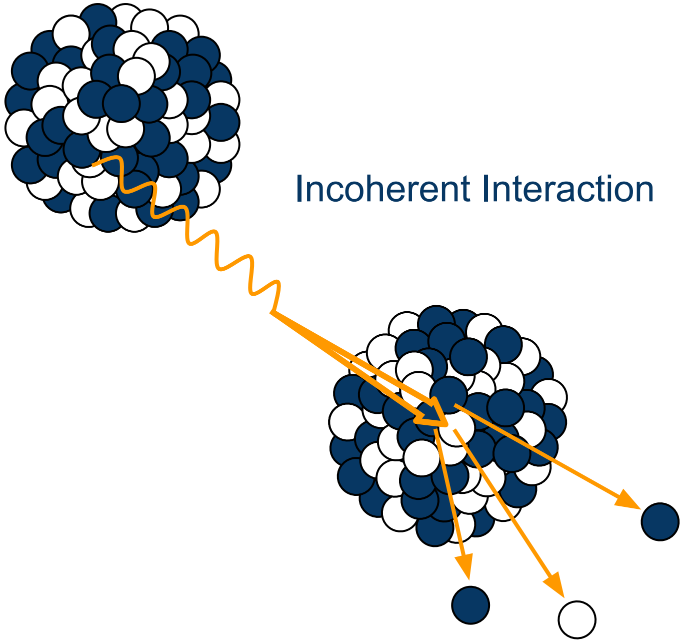

Incoherent Interaction

Coherent vs Incoherent Interactions

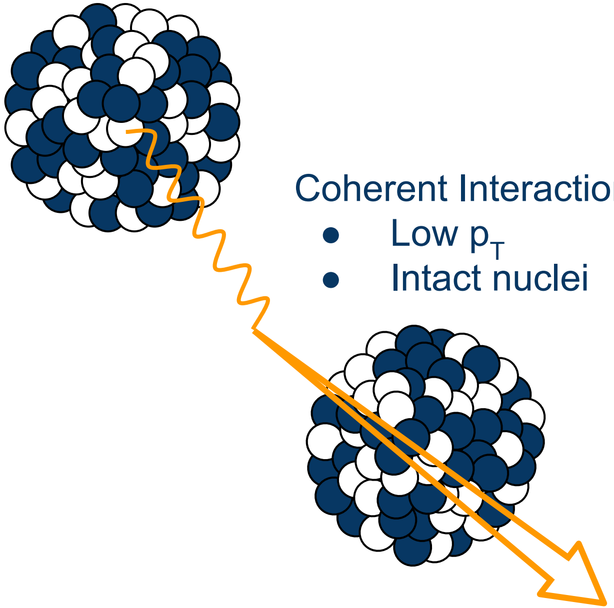

Coherent Interaction

- Low p_T
- Intact nuclei

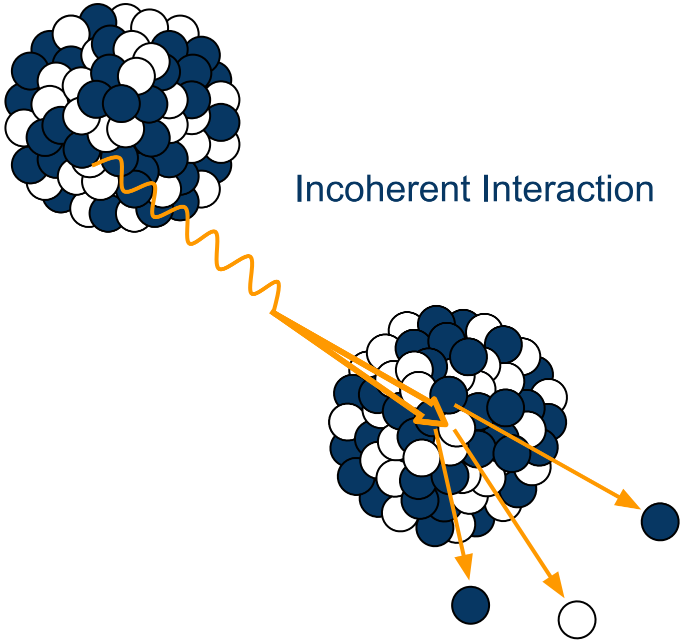

Incoherent Interaction

Coherent vs Incoherent Interactions

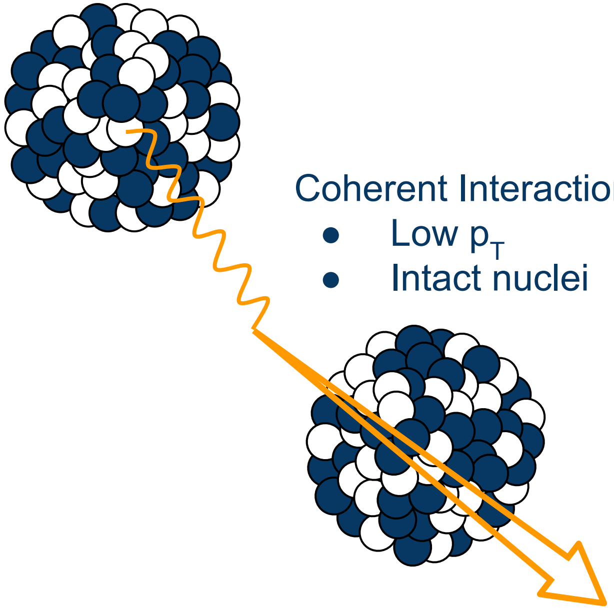

Coherent Interaction
- Low p_T
- Intact nuclei

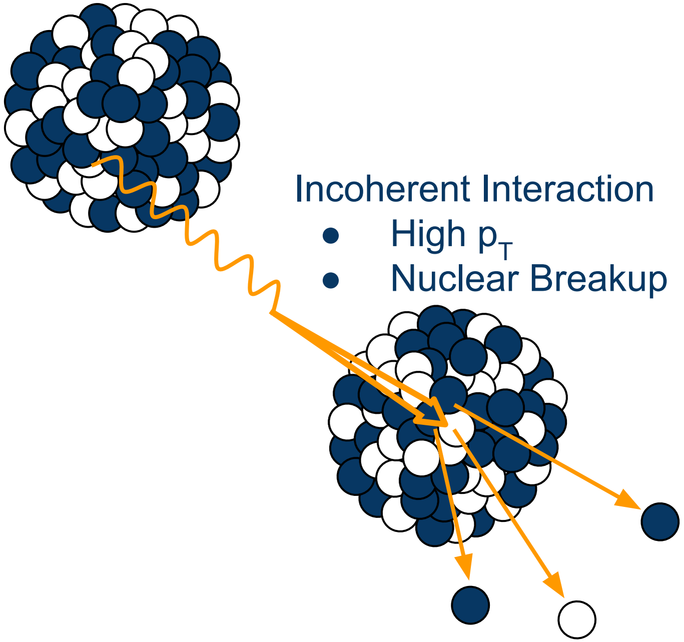

Incoherent Interaction
- High p_T
- Nuclear Breakup

Motivation

Motivation

- Understanding the di-pion spectrum
- Measured ρ parameters appear process dependent (tau decay, e^+e^-, photoproduction)
- low-mass spectroscopy: continuum, ω, high excitations, interference.

Why LHCb?

[2]

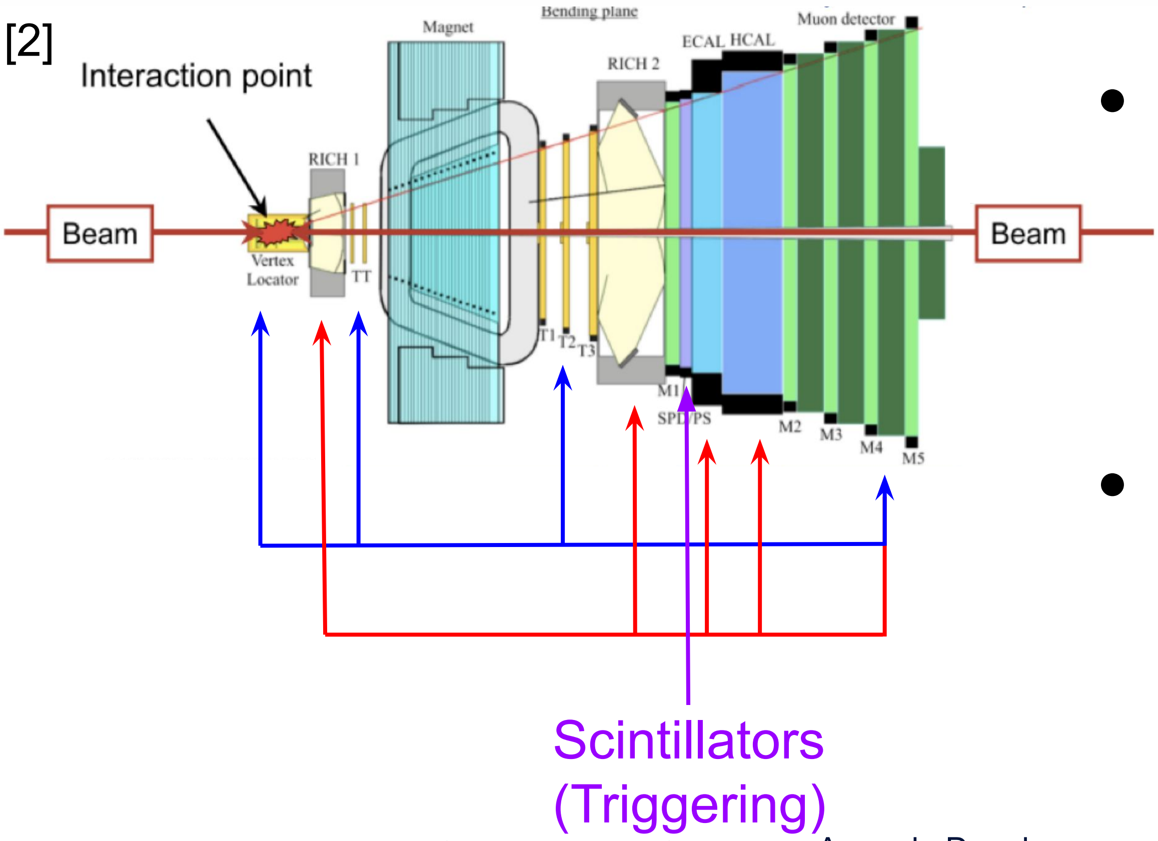

- A forward-arm spectrometer ($2 < \eta < 5$)
  - Unique acceptance and capabilities.
  - Constraints nPDFs down to $x \sim 10^{-6}$
- Precise Tracking and Full PID.
  - Mass resolution ($m_{\pi\pi}$) ~ 5 MeV.
  - Low background levels

HeRSCHeL Sub-Detector

[3]

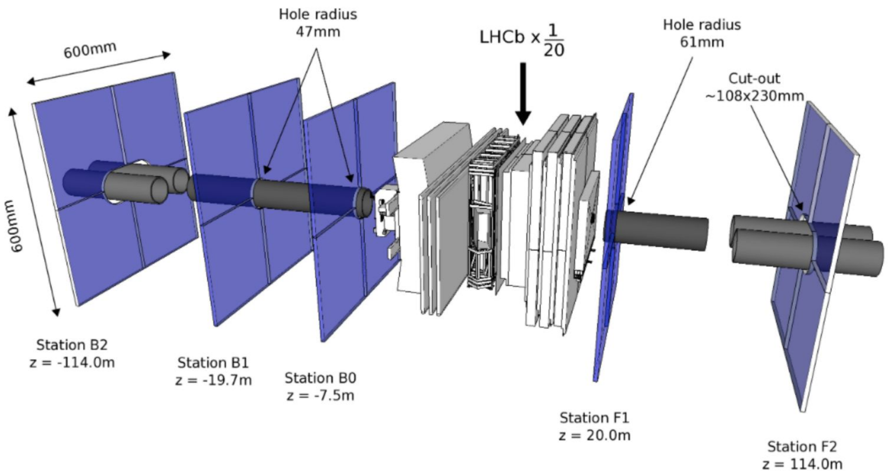

- HeRSCHeL
  - planes of scintillators up and downstream
  - extends coverage to $5 < |\eta| < 10$
- Enables distinction between coherent vs incoherent events due to ion dissociation

Di-Pion Lineshape

Data Selection

Data Used

- 2018 PbPb LHCb data
- $\sqrt{sNN}$ = 5.02 TeV
- Integrated luminosity: 228 ± 10 μb^{-1}

Selection Criteria

- Triggered Low Multiplicity Events (SPD < 50)
- Two oppositely charged tracks
- Fiducial region defined by $2.05 < y_{(parent)} < 4.9$, $p_{T(Track)} > 100$ Mev, and $2 < \eta_{Track} < 5$
- Invariant mass > 400 MeV
- Both tracks consistent with being a pion (using PID)
- Transverse momentum of the system < 100 MeV

Resultant Data

- Final sample contains ~12 million candidates

Backgrounds

LHCb-PAPER-2024-042

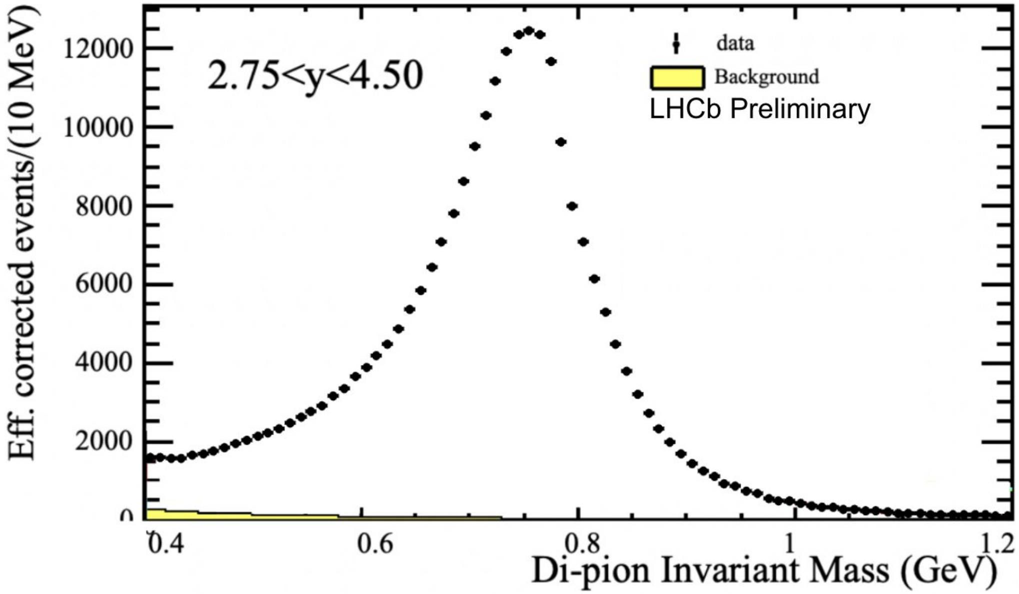

Backgrounds ~<1%

- **Gamma-gamma production**:
  - Diphoton production is peaked at low masses and low p_T
    - Hadron cross-section is an order of magnitude lower than leptons.
  - The shape of the $\gamma\gamma \rightarrow ee/\mu\mu$ backgrounds were determined by fitting events identified as electrons or muons.
  - The amount of contamination was determined using simulation, the shape is scaled by the ratio of missing leptons compared to the rate for tagging both.
  - Contamination from $\gamma\gamma \rightarrow ee$ and $\gamma\gamma \rightarrow \mu\mu$ processes ~0.5%.

Fitting the Invariant Mass Spectrum

- Söding basic
- Söding with ω (STAR)
- Söding with ω (H1)
- Söding with ω (H1) + form factor + continuum phase + ρ'

Söding basic

LHCb-PAPER-2024-042

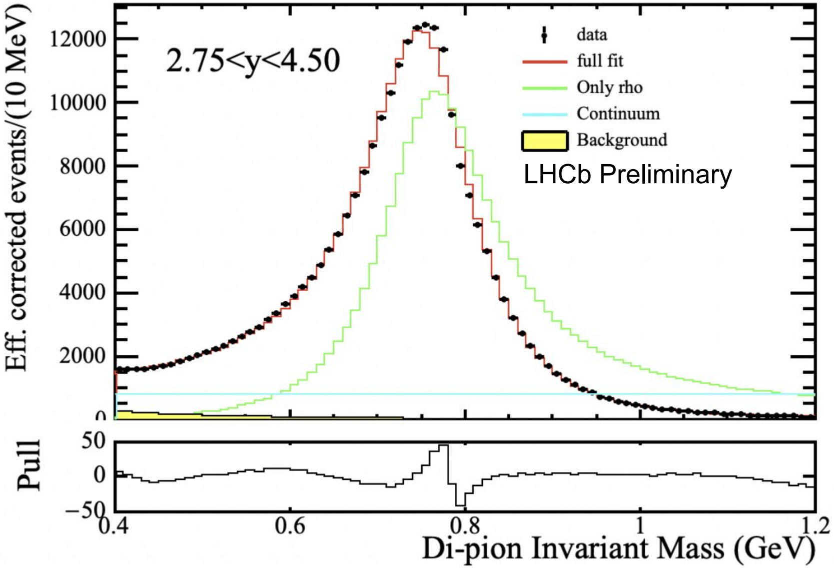

$$\mathcal{S}(M_{\pi\pi}) \propto \left| A \frac{\sqrt{M_{\pi\pi} M_\rho \Gamma}}{M_{\pi\pi}^2 - M_\rho^2 + i M_\rho \Gamma} + B \right|^2 \quad (1)$$

Experiment	Zeus [4]	H1 [5]	CMS [6]	ALICE [7]	LHCb Pb–Pb
Fit range [GeV]	[0.55,1.2]	[0.6,1.1]	[0.5,1.2]	[0.6,1.5]	[0.4,1.2]
M_ρ[MeV]	770 ± 2	769 ± 4	776 ± 1	$762^{+6.5}_{-3.8}$	771 ± 3
Γ_ρ [MeV]	146 ± 13	162 ± 8	154 ± 3	150^{+13}_{-7}	150 ± 4
$\lvert B/A \rvert$	0.70 ± 0.04	0.57 ± 0.09 [45]	0.50 ± 0.05	$0.50^{+0.10}_{-0.06}$	0.72 ± 0.04

Söding basic

LHCb-PAPER-2024-042

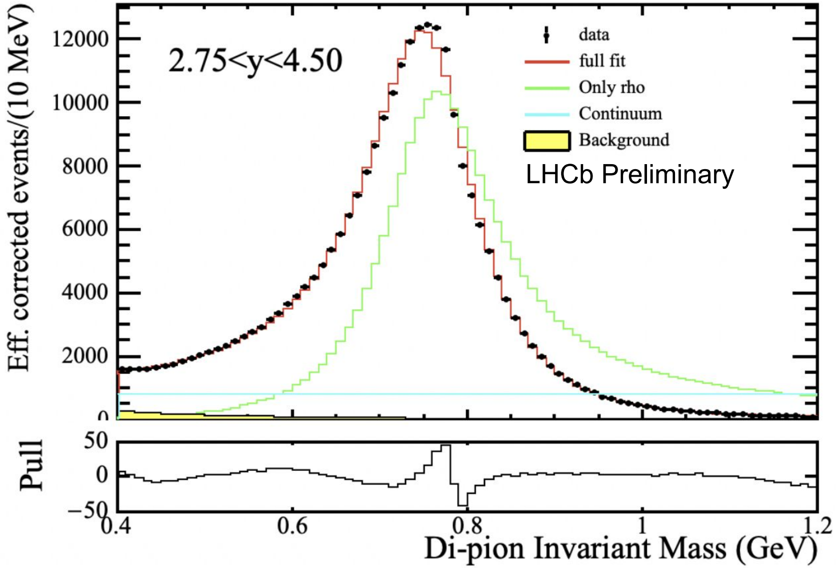

ρ resonance

$$\mathcal{S}(M_{\pi\pi}) \propto \left| A \frac{\sqrt{M_{\pi\pi} M_\rho \Gamma}}{M_{\pi\pi}^2 - M_\rho^2 + i M_\rho \Gamma} + B \right|^2 \quad (1)$$

Experiment	Zeus [4]	H1 [5]	CMS [6]	ALICE [7]	LHCb Pb–Pb
Fit range [GeV]	[0.55,1.2]	[0.6,1.1]	[0.5,1.2]	[0.6,1.5]	[0.4,1.2]
M_ρ[MeV]	770 ± 2	769 ± 4	776 ± 1	$762^{+6.5}_{-3.8}$	771 ± 3
Γ_ρ [MeV]	146 ± 13	162 ± 8	154 ± 3	150^{+13}_{-7}	150 ± 4
$\|B/A\|$	0.70 ± 0.04	0.57 ± 0.09 [45]	0.50 ± 0.05	$0.50^{+0.10}_{-0.06}$	0.72 ± 0.04

Söding basic

LHCb-PAPER-2024-042

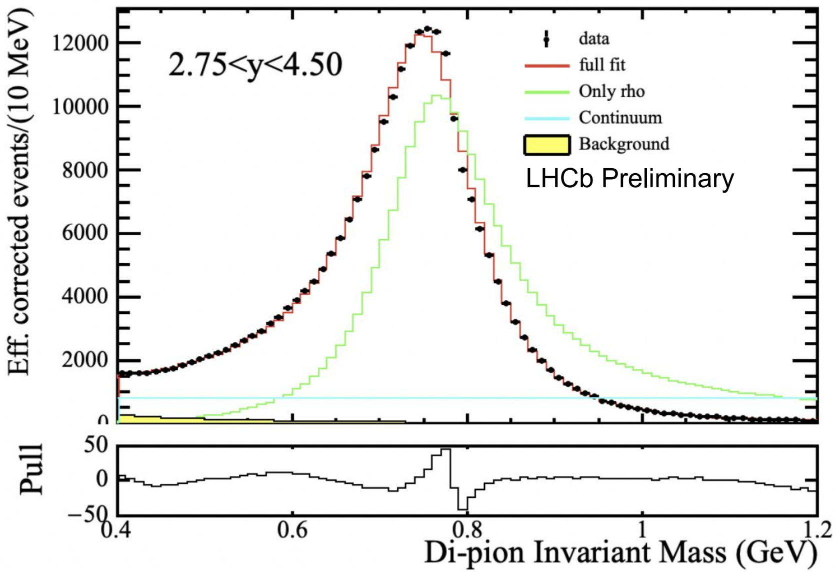

ρ resonance

$$\mathcal{S}(M_{\pi\pi}) \propto \left| A \frac{\sqrt{M_{\pi\pi} M_\rho \Gamma}}{M_{\pi\pi}^2 - M_\rho^2 + i M_\rho \Gamma} + B \right|^2 \quad (1)$$

flat continuum

Experiment	Zeus [4]	H1 [5]	CMS [6]	ALICE [7]	LHCb Pb–Pb
Fit range [GeV]	[0.55,1.2]	[0.6,1.1]	[0.5,1.2]	[0.6,1.5]	[0.4,1.2]
M_ρ [MeV]	770 ± 2	769 ± 4	776 ± 1	$762^{+6.5}_{-3.8}$	771 ± 3
Γ_ρ [MeV]	146 ± 13	162 ± 8	154 ± 3	150^{+13}_{-7}	150 ± 4
$\|B/A\|$	0.70 ± 0.04	0.57 ± 0.09 [45]	0.50 ± 0.05	$0.50^{+0.10}_{-0.06}$	0.72 ± 0.04

Söding basic

LHCb-PAPER-2024-042

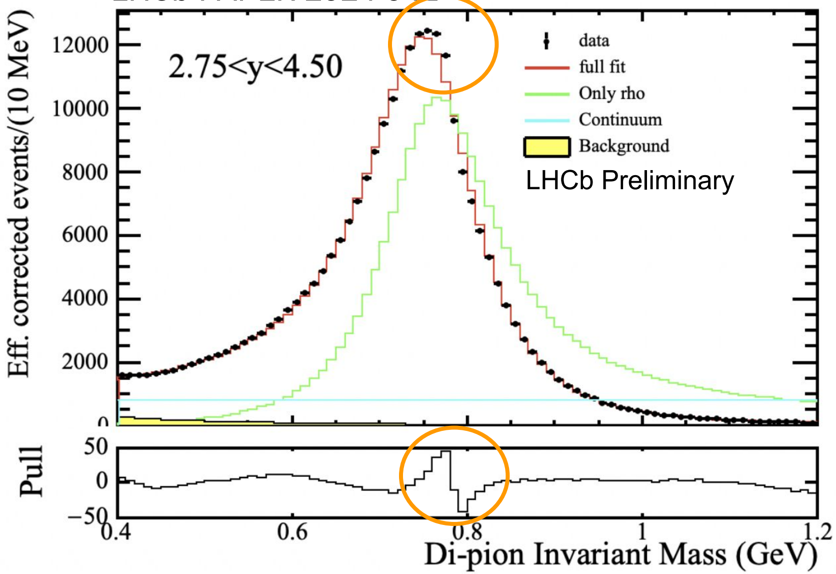

ρ resonance

flat continuum

$$\mathcal{S}(M_{\pi\pi}) \propto \left| A \frac{\sqrt{M_{\pi\pi} M_\rho \Gamma}}{M_{\pi\pi}^2 - M_\rho^2 + i M_\rho \Gamma} + B \right|^2 \quad (1)$$

Experiment	Zeus [4]	H1 [5]	CMS [6]	ALICE [7]	LHCb Pb–Pb
Fit range [GeV]	[0.55,1.2]	[0.6,1.1]	[0.5,1.2]	[0.6,1.5]	[0.4,1.2]
M_ρ[MeV]	770 ± 2	769 ± 4	776 ± 1	$762^{+6.5}_{-3.8}$	771 ± 3
Γ_ρ [MeV]	146 ± 13	162 ± 8	154 ± 3	150^{+13}_{-7}	150 ± 4
$\lvert B/A \rvert$	0.70 ± 0.04	0.57 ± 0.09 [45]	0.50 ± 0.05	$0.50^{+0.10}_{-0.06}$	0.72 ± 0.04

Söding + ω (STAR [8])

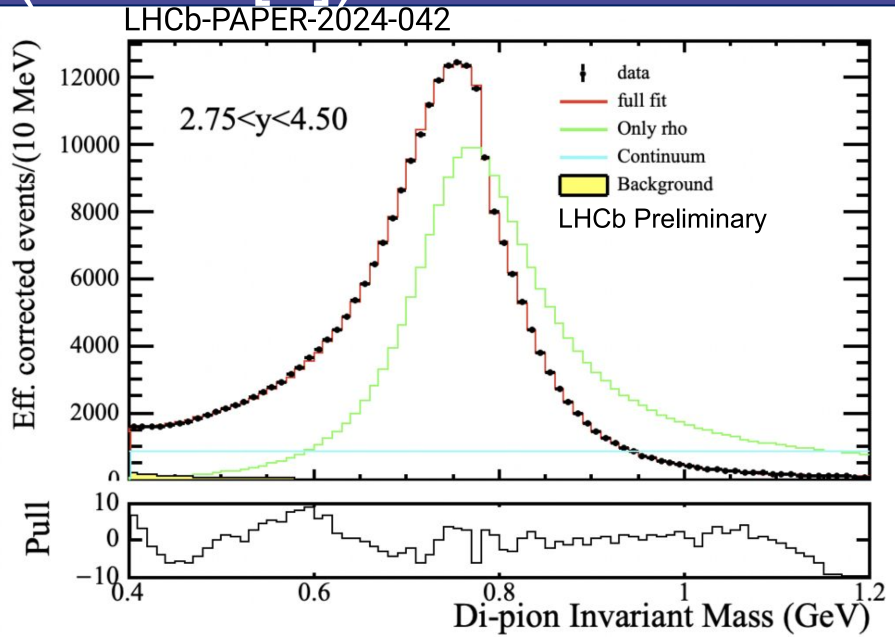

$$S = \left| A \frac{\sqrt{M_{\pi\pi} M_\rho \Gamma}}{M_{\pi\pi}^2 - M_\rho^2 + i M_\rho \Gamma} + B + C \exp(i\phi_\omega) \frac{\sqrt{M_{\pi\pi} M_\omega \Gamma_\omega}}{M_{\pi\pi}^2 - M_\omega^2 + i M_\omega \Gamma_\omega} \right|^2 \qquad (2)$$

Söding + ω (STAR [8])

LHCb-PAPER-2024-042

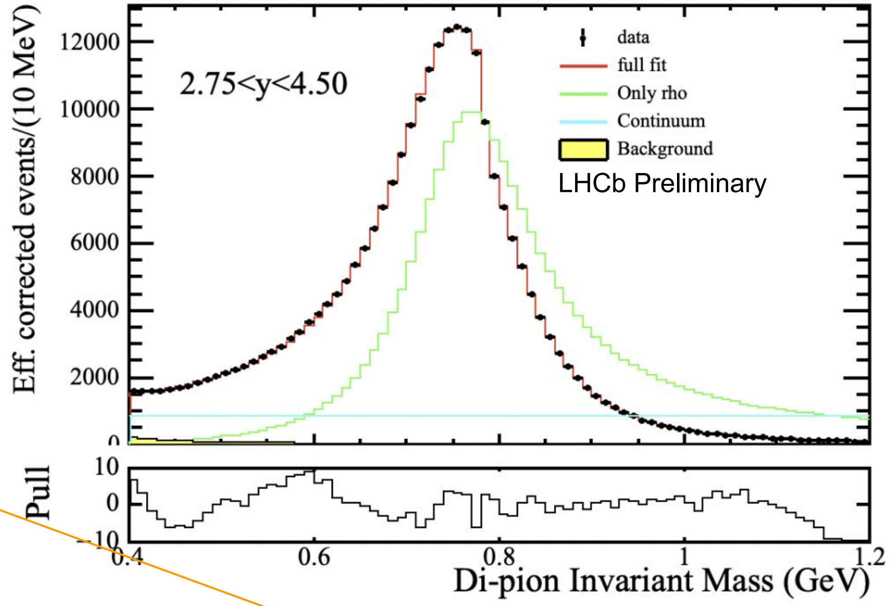

ω contribution

$$S = \left| A \frac{\sqrt{M_{\pi\pi} M_\rho \Gamma}}{M_{\pi\pi}^2 - M_\rho^2 + i M_\rho \Gamma} + B + C \exp(i\phi_\omega) \frac{\sqrt{M_{\pi\pi} M_\omega \Gamma_\omega}}{M_{\pi\pi}^2 - M_\omega^2 + i M_\omega \Gamma_\omega} \right|^2 \quad (2)$$

Söding + ω (STAR [8])

LHCb-PAPER-2024-042

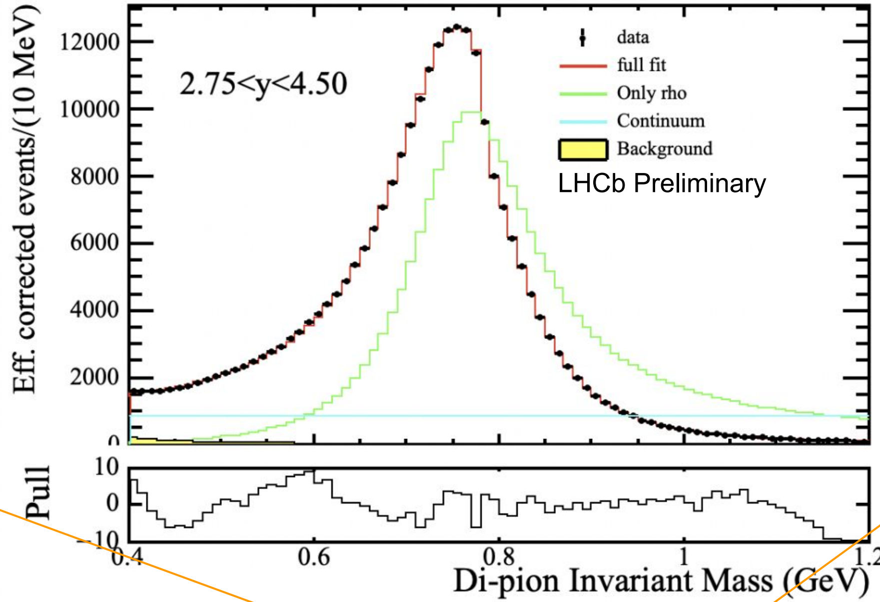

ω contribution

ω phase

$$S = \left| A \frac{\sqrt{M_{\pi\pi} M_\rho \Gamma}}{M_{\pi\pi}^2 - M_\rho^2 + i M_\rho \Gamma} + B + C \exp(i\phi_\omega) \frac{\sqrt{M_{\pi\pi} M_\omega \Gamma_\omega}}{M_{\pi\pi}^2 - M_\omega^2 + i M_\omega \Gamma_\omega} \right|^2 \quad (2)$$

Söding + ω (STAR [8])

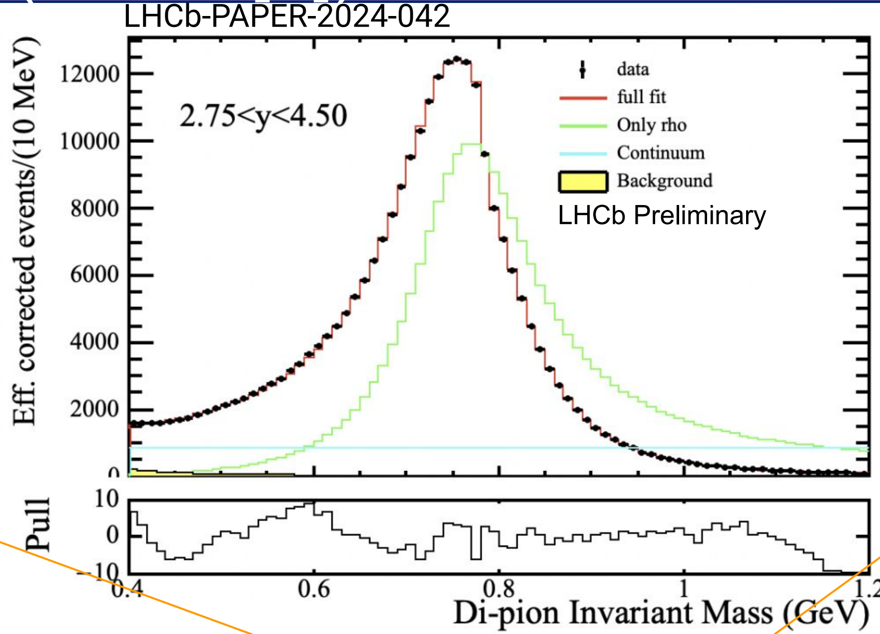

- ω mass a width are fixed to PDG values

ω contribution

ω phase

$$S = \left| A \frac{\sqrt{M_{\pi\pi} M_\rho \Gamma}}{M_{\pi\pi}^2 - M_\rho^2 + i M_\rho \Gamma} + B + C \exp(i\phi_\omega) \frac{\sqrt{M_{\pi\pi} M_\omega \Gamma_\omega}}{M_{\pi\pi}^2 - M_\omega^2 + i M_\omega \Gamma_\omega} \right|^2 \quad (2)$$

Söding + ω (STAR [8])

LHCb-PAPER-2024-042

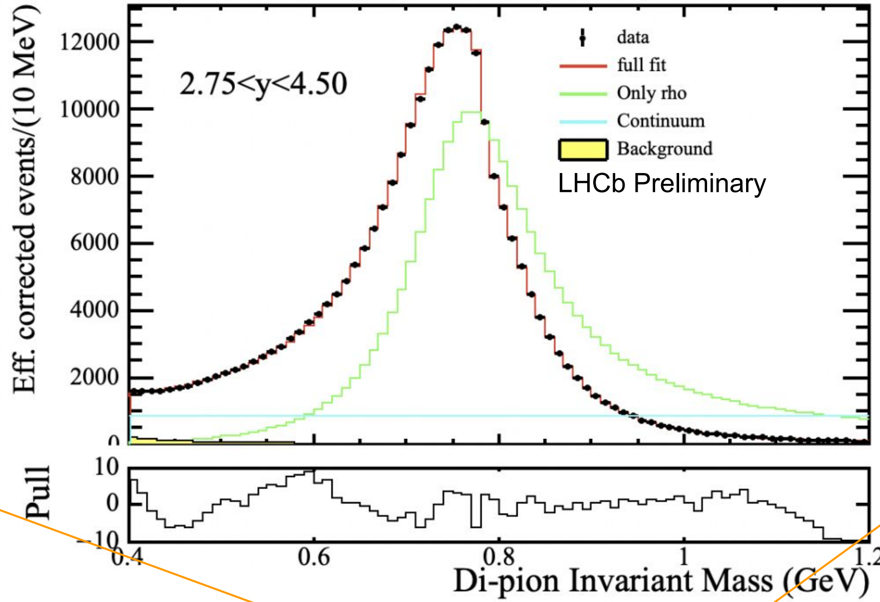

- ω mass a width are fixed to PDG values
- Small ω contribution, large effect from ω-ρ interference.

ω contribution

ω phase

$$S = \left| A \frac{\sqrt{M_{\pi\pi} M_\rho \Gamma}}{M_{\pi\pi}^2 - M_\rho^2 + i M_\rho \Gamma} + B + C \exp(i\phi_\omega) \frac{\sqrt{M_{\pi\pi} M_\omega \Gamma_\omega}}{M_{\pi\pi}^2 - M_\omega^2 + i M_\omega \Gamma_\omega} \right|^2 \quad (2)$$

Söding + ω (STAR [8])

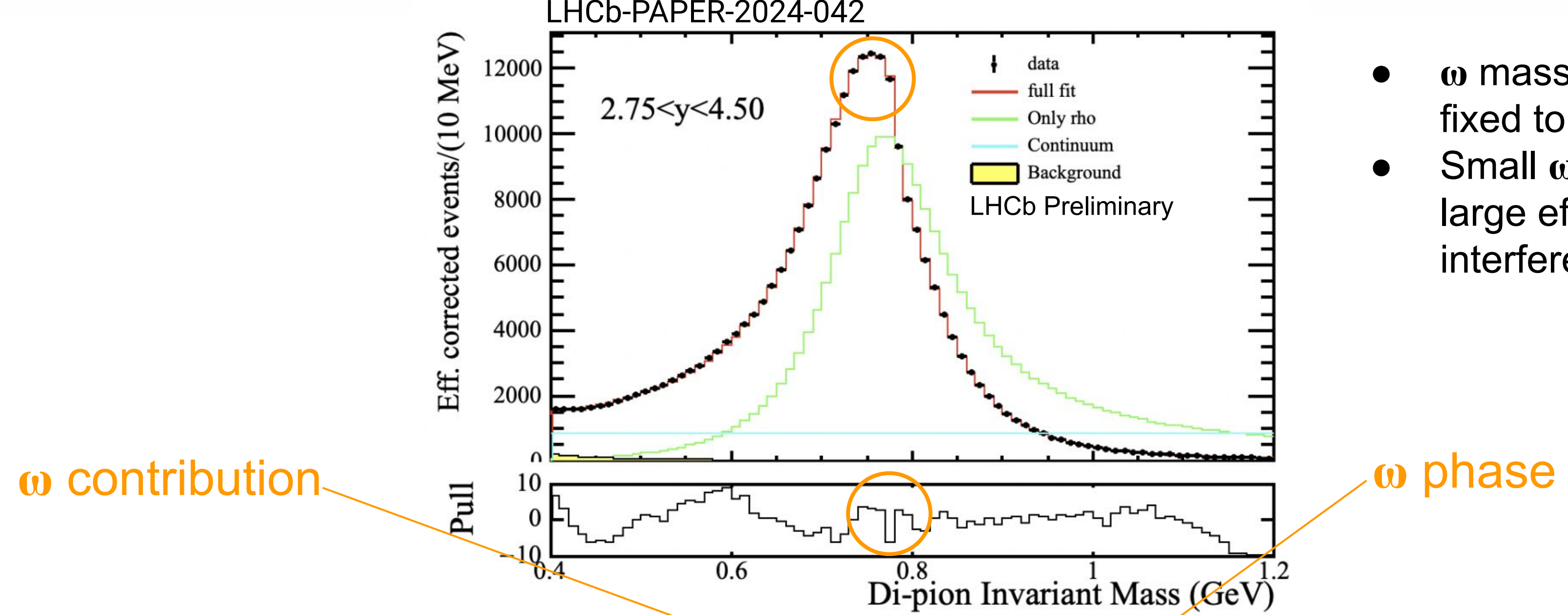

- ω mass a width are fixed to PDG values
- Small ω contribution, large effect from ω-ρ interference.

$$S = \left| A \frac{\sqrt{M_{\pi\pi} M_\rho \Gamma}}{M_{\pi\pi}^2 - M_\rho^2 + i M_\rho \Gamma} + B + C \exp(i\phi_\omega) \frac{\sqrt{M_{\pi\pi} M_\omega \Gamma_\omega}}{M_{\pi\pi}^2 - M_\omega^2 + i M_\omega \Gamma_\omega} \right|^2 \quad (2)$$

Söding + ω (H1 [9])

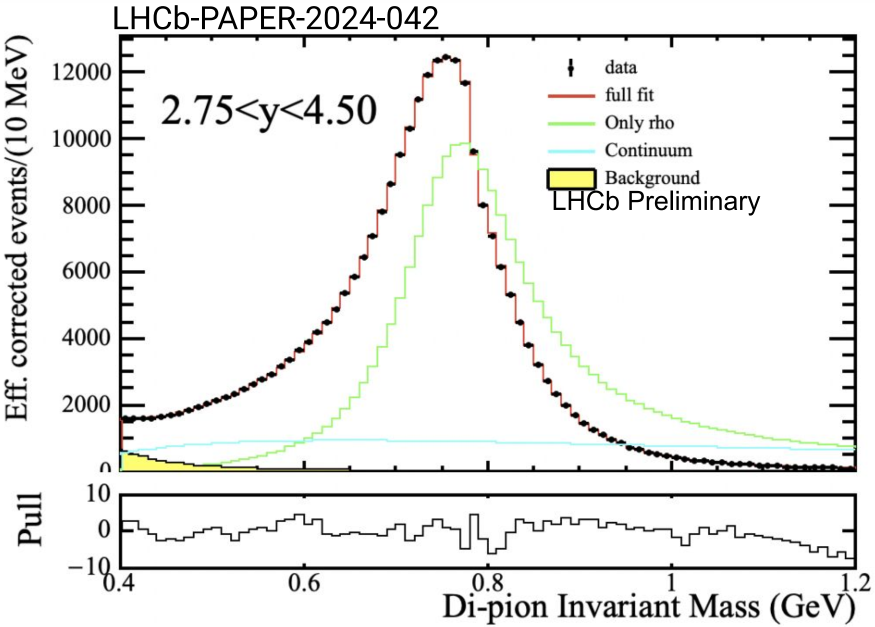

$$S = \frac{q^3(m_{\pi\pi})}{q^3(m_\rho)} \left| \mathcal{BW}_\rho(m_{\pi\pi}) \left(1 + C \exp(i\phi_\omega) \frac{m_{\pi\pi}^2}{m_\omega^2} \mathcal{BW}_\omega(m_{\pi\pi}) \right) + \frac{B}{(m_{\pi\pi}^2 - 4m_\pi^2 + \Lambda^2)^\delta} \right|^2 \quad (3)$$

Söding + ω (H1 [9])

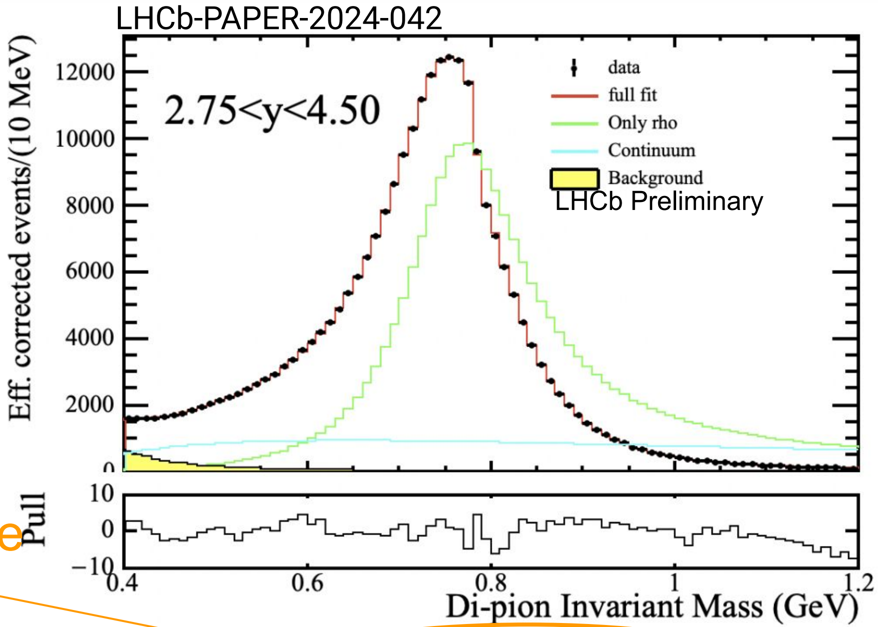

Modified ω phase/interference

$$S = \frac{q^3(m_{\pi\pi})}{q^3(m_\rho)} \left| \mathcal{BW}_\rho(m_{\pi\pi}) \left(1 + C \exp(i\phi_\omega) \frac{m_{\pi\pi}^2}{m_\omega^2} \mathcal{BW}_\omega(m_{\pi\pi}) \right) + \frac{B}{(m_{\pi\pi}^2 - 4m_\pi^2 + \Lambda^2)^\delta} \right|^2 \quad (3)$$

Söding + ω (H1 [9])

LHCb-PAPER-2024-042

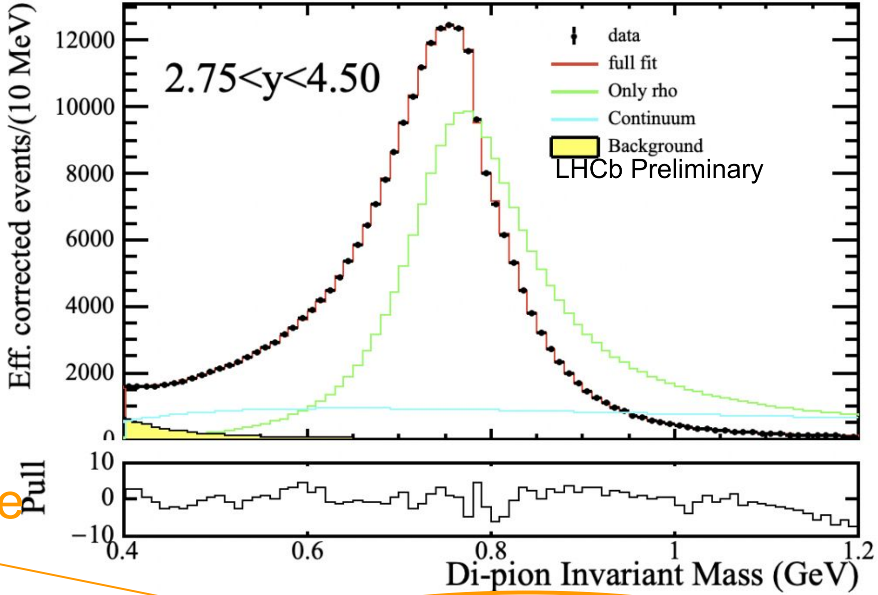

Modified ω phase/interference

Modified continuum

$$S = \frac{q^3(m_{\pi\pi})}{q^3(m_\rho)} \left| \mathcal{BW}_\rho(m_{\pi\pi}) \left(1 + C\exp(i\phi_\omega)\frac{m_{\pi\pi}^2}{m_\omega^2}\mathcal{BW}_\omega(m_{\pi\pi})\right) + \frac{B}{(m_{\pi\pi}^2 - 4m_\pi^2 + \Lambda^2)^\delta}\right|^2 \quad (3)$$

Söding + ω (H1 [9])

LHCb-PAPER-2024-042

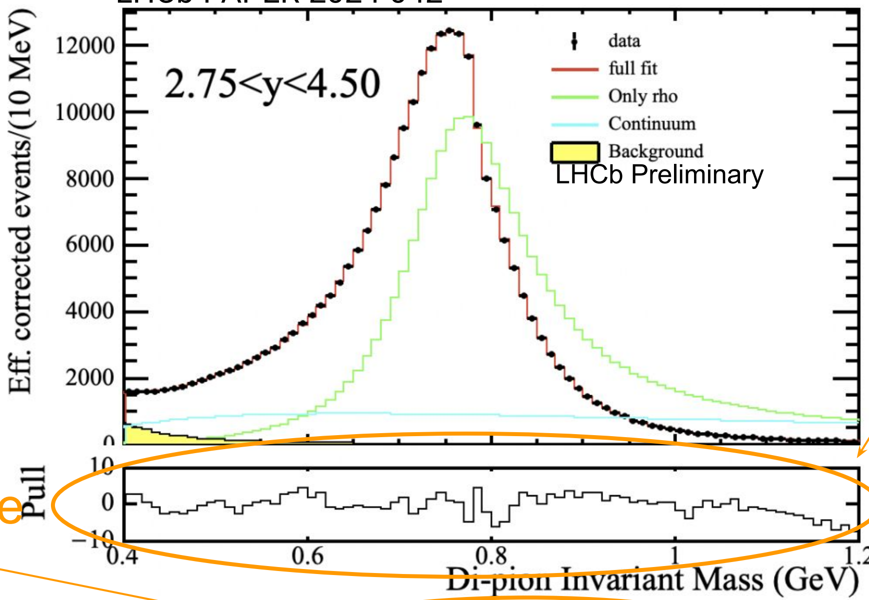

Fewer Deviations on Pull

Modified ω phase/interference

Modified continuum

$$S = \frac{q^3(m_{\pi\pi})}{q^3(m_\rho)} \left| \mathcal{BW}_\rho(m_{\pi\pi}) \left(1 + C\exp(i\phi_\omega)\frac{m_{\pi\pi}^2}{m_\omega^2}\mathcal{BW}_\omega(m_{\pi\pi})\right) + \frac{B}{(m_{\pi\pi}^2 - 4m_\pi^2 + \Lambda^2)^\delta}\right|^2 \quad (3)$$

Fit Results

LHCb Preliminary LHCb-PAPER-2024-042	LHCb (Star eq. 2)	LHCb (H1 eq. 3)	STAR [8]	H1 [9]
M_ρ[MeV]	774 ± 3	776 ± 3	776.2 ± 0.2	771 ± 3
Γ_ρ [MeV]	156 ± 3	153 ± 3	156 ± 1	151 ± 3
$\|B/A\|$	0.73 ± 0.03	$0.19 \pm .02$	0.79 ± 0.08	0.19 ± 0.04
ϕ_ω[rad]	1.36 ± 0.03	$-0.23 \pm .04$	1.46 ± 0.11	-0.5 ± 0.3
$\|C/A\|$	0.34 ± 0.03	$0.18 \pm .01$	0.36 ± 0.05	0.17 ± 0.02
Λ[MeV]	-	366 ± 110		180 ± 590
δ	-	$1.07 \pm .11$	-	0.76 ± 0.35

But What about Masses > 1.2 GeV?

LHCb-PAPER-2024-042

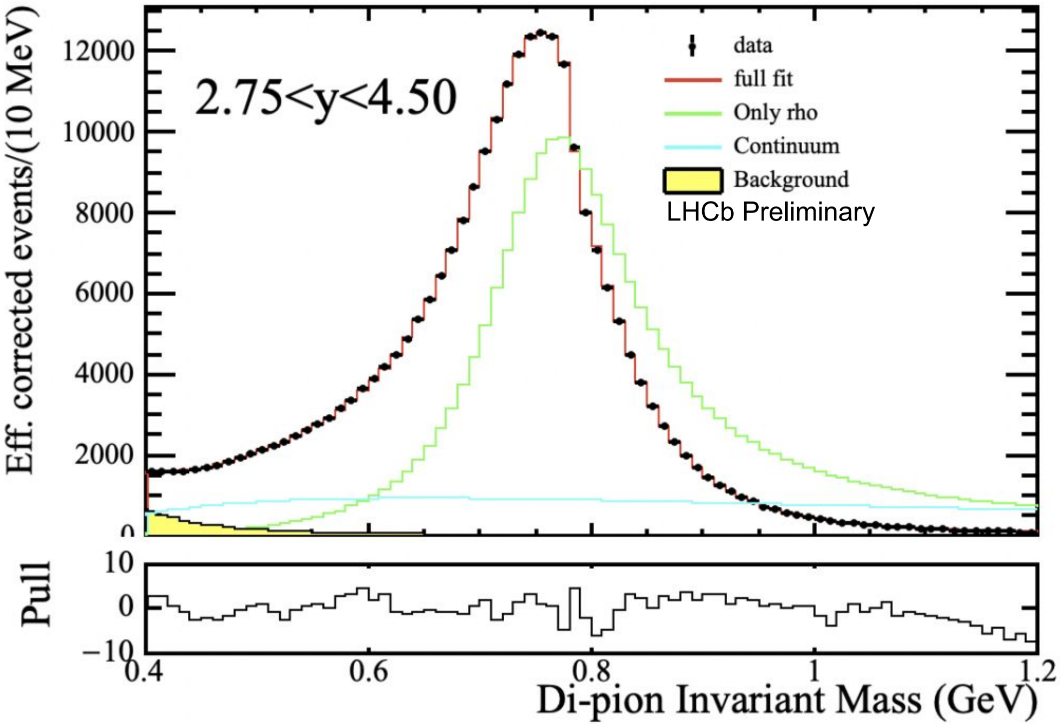

Extended Frame

LHCb-PAPER-2024-042

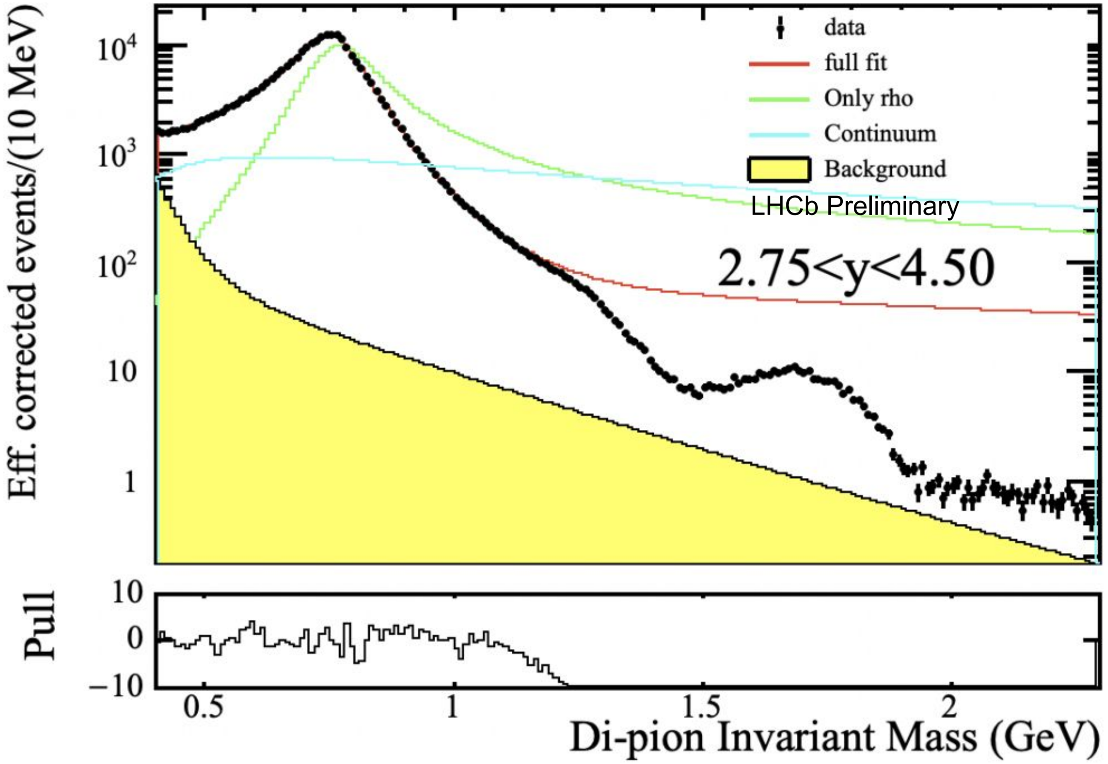

- Data at high mass falls well below fit
- Does not account for clear structure around 1.7 GeV

Söding + ω (H1) + form factor + continuum phase + ρ'

LHCb-PAPER-2024-042

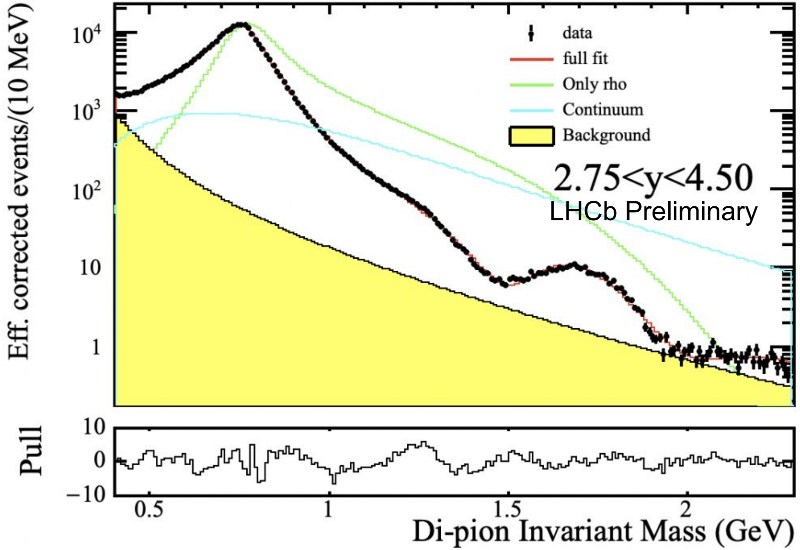

$$S = \frac{q^3(m_{\pi\pi})}{q^3(m_\rho)} \left| \exp\left(-\left(\frac{m_{\pi\pi}^2 - m_\rho^2}{\Delta^2}\right)^2\right) \mathcal{BW}_\rho(m_{\pi\pi}) \left(1 + C\exp(i\phi_\omega)\frac{m_{\pi\pi}^2}{m_\omega^2}\mathcal{BW}_\omega(m_{\pi\pi})\right) \right. \quad (6)$$

$$\left. + \frac{B\exp(i\phi_c)}{(m_{\pi\pi}^2 - 4m_\pi^2 + \Lambda^2)^\delta} + D\exp(i\phi_{\rho'})\mathcal{BW}_{\rho'} \right|^2 \quad (4)$$

Fit the data with:

- Added form factor
- High-mass Breit-Wigner term
- Interference from continuum

Alternative parameterizations are possible

Söding + ω (H1) + form factor + continuum phase + ρ’

LHCb-PAPER-2024-042

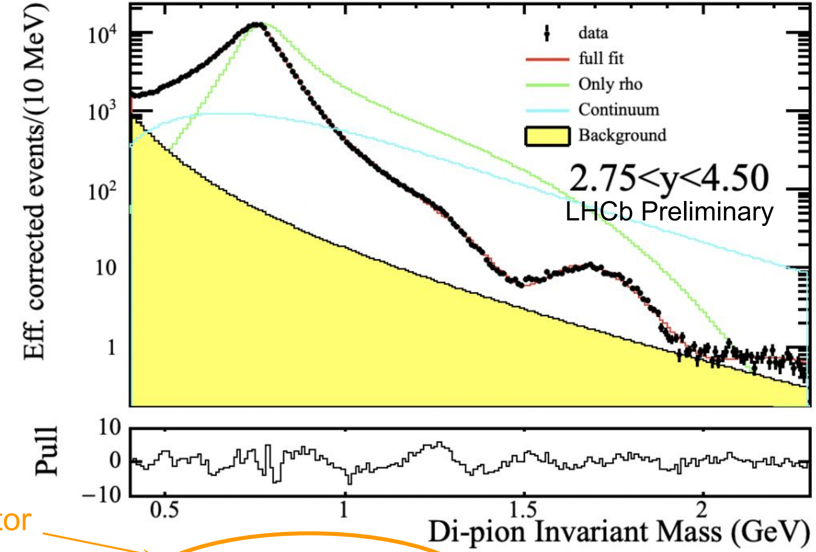

Form Factor

$$S = \frac{q^3(m_{\pi\pi})}{q^3(m_\rho)} \left| \exp\left(-\left(\frac{m_{\pi\pi}^2 - m_\rho^2}{\Delta^2}\right)^2\right) \mathcal{BW}_\rho(m_{\pi\pi}) \left(1 + C\exp(i\phi_\omega)\frac{m_{\pi\pi}^2}{m_\omega^2}\mathcal{BW}_\omega(m_{\pi\pi})\right) \right. \quad (6)$$

$$\left. + \frac{B\exp(i\phi_c)}{(m_{\pi\pi}^2 - 4m_\pi^2 + \Lambda^2)^\delta} + D\exp(i\phi_{\rho'})\mathcal{BW}_{\rho'} \right|^2 \quad (4)$$

Fit the data with:

- Added form factor
- High-mass Breit-Wigner term
- Interference from continuum

Alternative parameterizations are possible

Söding + ω (H1) + form factor + continuum phase + ρ'

LHCb-PAPER-2024-042

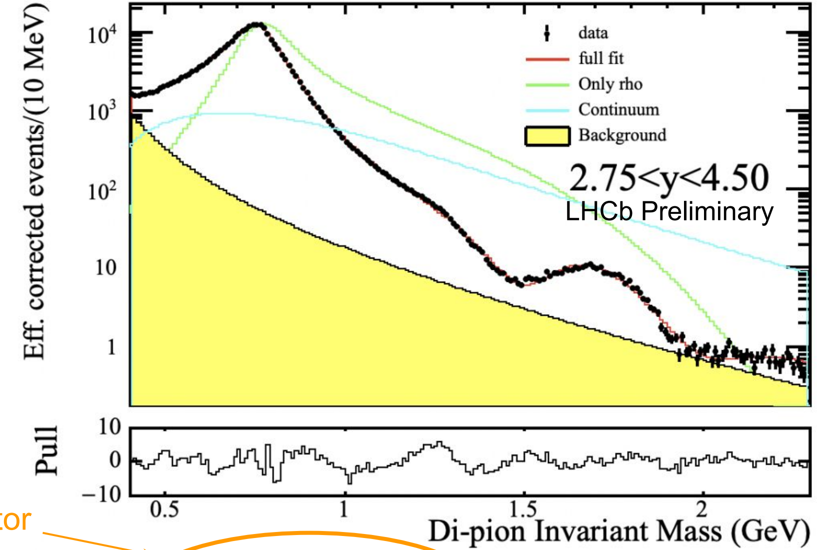

Fit the data with:

- Added form factor
- High-mass Breit-Wigner term
- Interference from continuum

Alternative parameterizations are possible

Form Factor

$$S = \frac{q^3(m_{\pi\pi})}{q^3(m_\rho)} \left| \exp\left(-\left(\frac{m_{\pi\pi}^2 - m_\rho^2}{\Delta^2}\right)^2\right) \mathcal{BW}_\rho(m_{\pi\pi}) \left(1 + C\exp(i\phi_\omega)\frac{m_{\pi\pi}^2}{m_\omega^2}\mathcal{BW}_\omega(m_{\pi\pi})\right) \right. \quad (6)$$

$$\left. + \frac{B\exp(i\phi_c)}{(m_{\pi\pi}^2 - 4m_\pi^2 + \Lambda^2)^\delta} + D\exp(i\phi_{\rho'})\mathcal{BW}_{\rho'} \right|^2 \quad (4)$$

ρ' resonance

Söding + ω (H1) + form factor + continuum phase + ρ’

LHCb-PAPER-2024-042

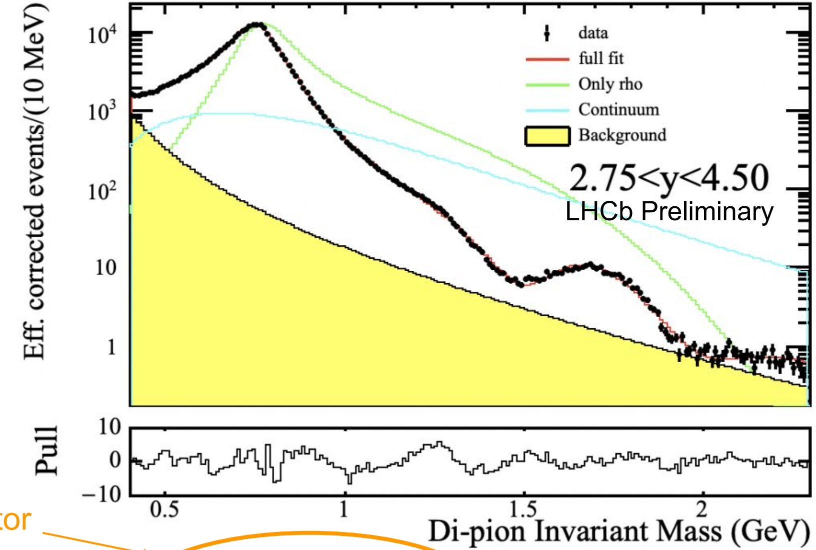

Fit the data with:

- Added form factor
- High-mass Breit-Wigner term
- Interference from continuum

Alternative parameterizations are possible

Form Factor

$$S = \frac{q^3(m_{\pi\pi})}{q^3(m_\rho)}\left| \exp\left(-\left(\frac{m_{\pi\pi}^2 - m_\rho^2}{\Delta^2}\right)^2\right)\mathcal{BW}_\rho(m_{\pi\pi})\left(1 + C\exp(i\phi_\omega)\frac{m_{\pi\pi}^2}{m_\omega^2}\mathcal{BW}_\omega(m_{\pi\pi})\right) \right. \quad (6)$$

$$\left. + \frac{B\exp(i\phi_c)}{(m_{\pi\pi}^2 - 4m_\pi^2 + \Lambda^2)^\delta} + D\exp(i\phi_{\rho'})\mathcal{BW}_{\rho'}\right|^2 \quad (4)$$

Continuum Phase Shift

ρ’ resonance

Söding + ω (H1) + form factor + continuum phase + ρ’

LHCb-PAPER-2024-042

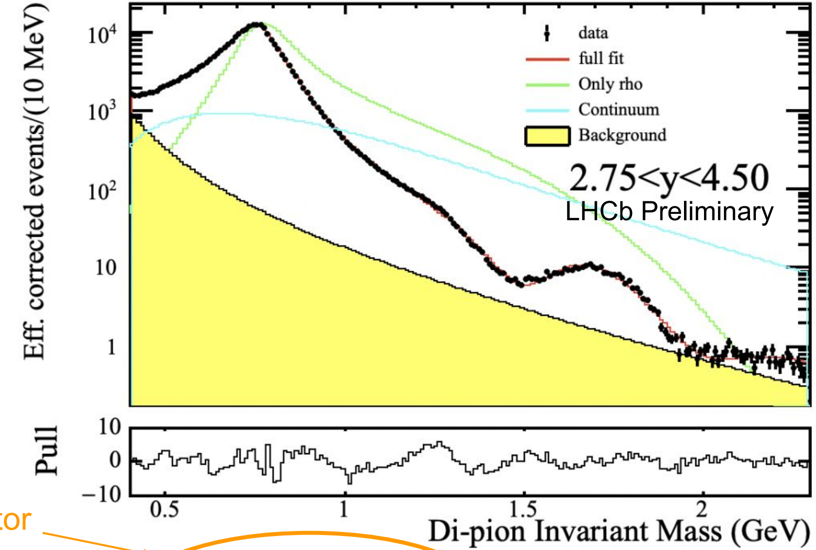

	fit to eq. 4
M_ρ[MeV]	777.0±0.1
Γ_ρ [MeV]	152.2±0.2
ϕ_c	-0.52±0.02
$\lvert B/A\rvert$	1.1 ± 0.1
$\phi_\omega[rad]$	-0.14±.01
$\lvert C/A\rvert$	0.160 ± 0.002
Λ[MeV]	1.04 ± 0.02
δ	2.98±0.05
Δ[MeV]	1.49±0.01
$\lvert D/A\rvert$	0.0124 ± 0.0003,
$M_{\rho'}$[MeV]	1620 ± 8
$\Gamma_{\rho'}$[MeV]	462 ± 10
$\phi_{\rho'}$	−0.26 ± 0.03

Form Factor

$$S = \frac{q^3(m_{\pi\pi})}{q^3(m_\rho)} \left| \exp\left(-\left(\frac{m_{\pi\pi}^2 - m_\rho^2}{\Delta^2}\right)^2\right) \mathcal{BW}_\rho(m_{\pi\pi}) \left(1 + C\exp(i\phi_\omega)\frac{m_{\pi\pi}^2}{m_\omega^2}\mathcal{BW}_\omega(m_{\pi\pi})\right) + \frac{B\exp(i\phi_c)}{(m_{\pi\pi}^2 - 4m_\pi^2 + \Lambda^2)^\delta} + D\exp(i\phi_{\rho'})\mathcal{BW}_{\rho'} \right|^2 \quad (4)$$

Continuum Phase Shift

ρ’ resonance

Söding + ω (H1) + form factor + continuum phase + ρ’

LHCb-PAPER-2024-042

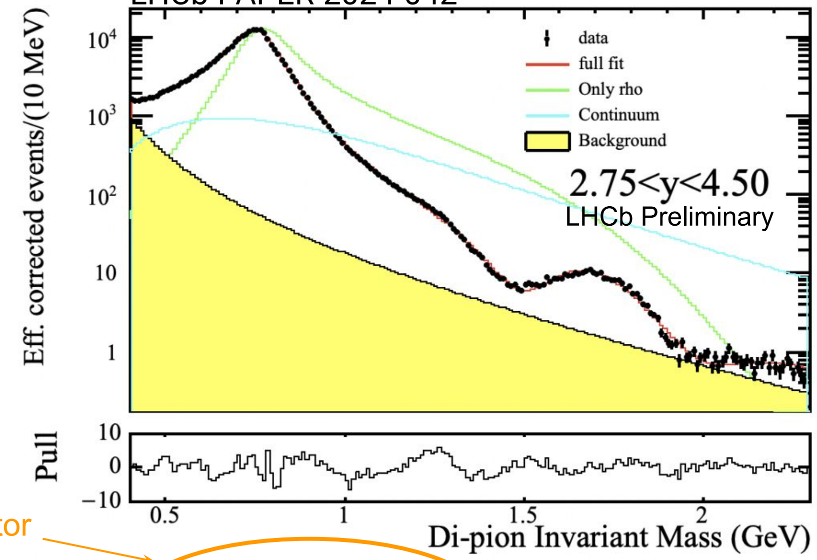

Form Factor

Continuum Phase Shift

ρ’ resonance

$$S = \frac{q^3(m_{\pi\pi})}{q^3(m_\rho)} \left| \exp\left(-\left(\frac{m_{\pi\pi}^2 - m_\rho^2}{\Delta^2}\right)^2\right) \mathcal{BW}_\rho(m_{\pi\pi}) \left(1 + C\exp(i\phi_\omega)\frac{m_{\pi\pi}^2}{m_\omega^2}\mathcal{BW}_\omega(m_{\pi\pi})\right) + \frac{B\exp(i\phi_c)}{(m_{\pi\pi}^2 - 4m_\pi^2 + \Lambda^2)^\delta} + D\exp(i\phi_{\rho'})\mathcal{BW}_{\rho'} \right|^2 \quad (4)$$

	fit to eq. 4
M_ρ[MeV]	777.0±0.1
Γ_ρ [MeV]	152.2±0.2
ϕ_c	-0.52±0.02
$\lvert B/A \rvert$	1.1 ± 0.1
$\phi_\omega[rad]$	-0.14±.01
$\lvert C/A \rvert$	0.160 ± 0.002
Λ[MeV]	1.04 ± 0.02
δ	2.98±0.05
Δ[MeV]	1.49±0.01
$\lvert D/A \rvert$	0.0124 ± 0.0003,
$M_{\rho'}$[MeV]	1620 ± 8 }
$\Gamma_{\rho'}$[MeV]	462 ± 10 }
$\phi_{\rho'}$	−0.26 ± 0.03

} = Strongly Model Dependent

Conclusions and Outlook

Conclusions

- Very clean sample with approximately 1% background
- Extended measurement range to 0.4 - 2.3 GeV
  - Previous results from 0.6-1.0 GeV (H1 [9]) and 0.6-1.3 GeV (STAR [8])
- Distinct and well-resolved resonance observed at 1.7 GeV
- Full description of the di-pion spectrum requires phenomenological input.

Outlook

- Will feed into cross section measurements.

References

[1] M. Davier, A. Hoecker, B. Malaescu, and Z. Zhang, Reevaluation of the hadronic 385 vacuum polarisation contributions to the Standard Model predictions of the muon g − 2 and α(m2 Z 386) using newest hadronic cross-section data, Eur. Phys. J. C 77 (2017) 387 827, arXiv:1706.09436.

[2] Int. J. Mod. Phys. A 30 (2015) 1530022
[3] JINST 13 (2018) no.04, P04017

[4] ZEUS, J. Breitweg et al., Elastic and proton dissociative ρ 0 451 photoproduction at HERA, 452 Eur. Phys. J. C 2 (1998) 247, arXiv:hep-ex/9712020.

[5] H1, F. D. Aaron et al., Diffractive Electroproduction of rho and phi Mesons at HERA, 454 JHEP 05 (2010) 032, arXiv:0910.5831.

[6] CMS, A. M. Sirunyan et al., Measurement of exclusive ρ(770)0 455 photoproduction in ultraperipheral pPb collisions at √ 456 sNN = 5.02 TeV, Eur. Phys. J. C 79 (2019) 702, 457 arXiv:1902.01339.

[7] ALICE, J. Adam et al., Coherent ρ 0 400 photoproduction in ultra-peripheral Pb-Pb collisions at √ 401 sNN = 2.76 TeV, JHEP 09 (2015) 095, arXiv:1503.09177.

[8] STAR, L. Adamczyk et al., Coherent diffractive photoproduction of ρ 394 0mesons on gold 395 nuclei at 200 GeV/nucleon-pair at the Relativistic Heavy Ion Collider, Phys. Rev. C 396 96 (2017) 054904, arXiv:1702.07705.

[9] H1, V. Andreev et al., Measurement of Exclusive π +π − and ρ 388 0 Meson Photoproduction 389 at HERA, Eur. Phys. J. C 80 (2020) 1189, arXiv:2005.14471.

[10] ALICE collaboration, Coherent photoproduction of 0 vector mesons in ultra-peripheral Pb-Pb collisions at √ sNN = 5.02 TeV, JHEP 06 (2020) 035 [2002.10897].

Thank You

back-up

Alice ρ UPC in PbPb [10]

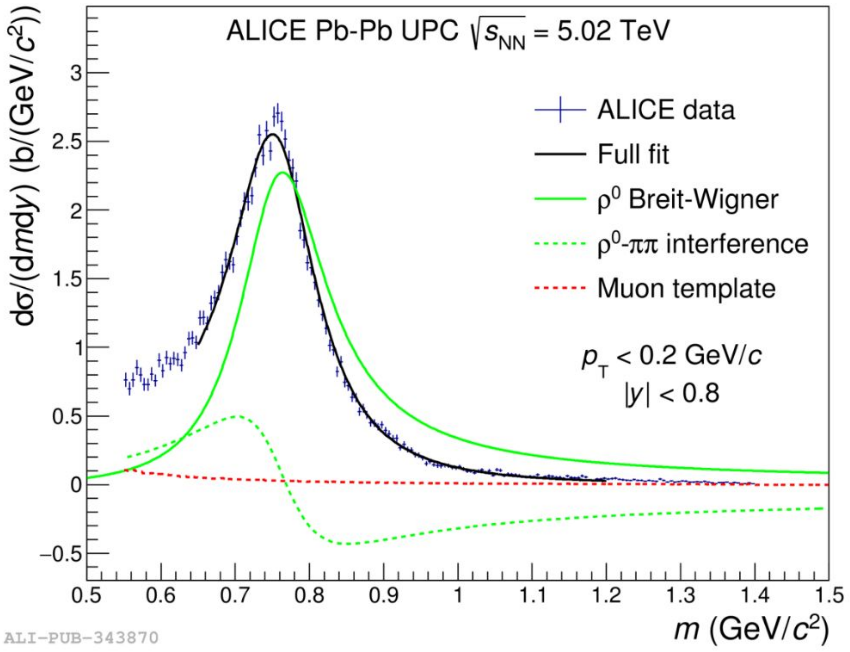

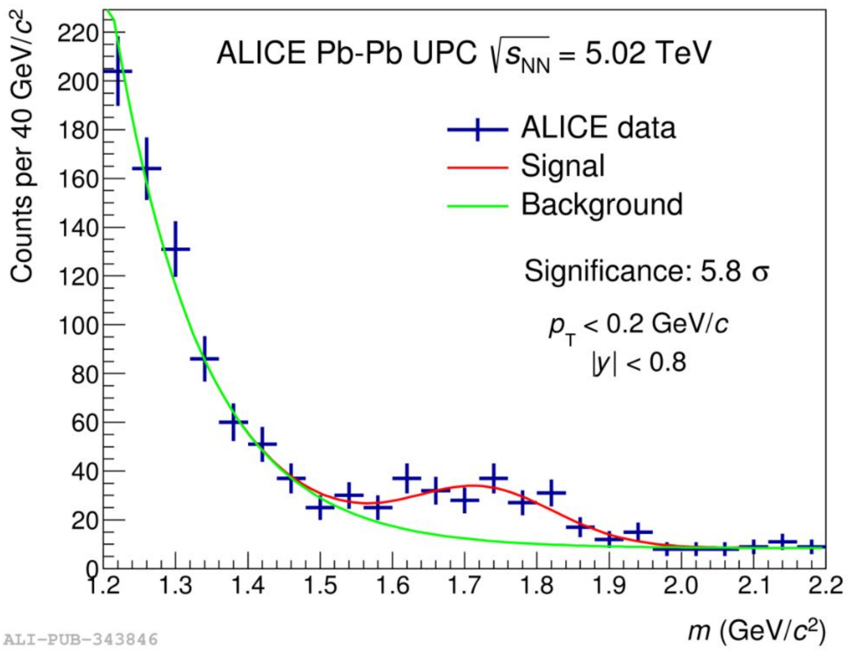

What is the Structure?

ALICE fitted an enhancement in this region with a Gaussian and obtained a mass of 1725 ± 17 MeV and a width of 143 ± 21 MeV compatible with the ρ(1700) while STAR, with a similar fit, obtained a mass of 1653 ± 10 MeV and a width of 164 ± 15 MeV, compatible with the spin-3 ρ3(1690).